

This document contains the responses to the anonymous referees #1 and #2 as well as a marked-up version of the manuscript showing the changes made to the original version.

Author's response to Anonymous Referee #1:

The authors thank the referee very much for the time and effort to review our manuscript and for the valuable comments. Please find our responses below. The original comments are stated in **bold** while our responses follow in plain text. Thank you very much.

Major comments:

P3, l10-11, Eq 5 : a space average is applied to the incoming flow measurements, arguing that “This approach is more appropriate to describe the wind speed affecting the rotor than a single point measurement”. Please elaborate your argumentation.

There are two reasons to use the space averaged wind speed to describe the inflow conditions at the rotor's position.

1. Due to the rotor's rotation, the turbine is affected by the whole wind field across the rotor swept area. A single point measurement might therefore not capture important flow characteristics affecting the rotor on other positions within the rotor swept area. In numerous recent studies a rotor effective wind speed for inflow descriptions and advanced control strategies is used to capture the actual wind speed affecting the rotor [1, 2].

Based on the data of the three hot wires, we investigated whether the space averaging shows different increment statistics compared to the single point measurements. As Fig. 1 of this reply shows, there is no significant difference regarding the intermittency of the increment PDF. The small deviations, especially of the center hot wire u_1 , might be explained by the second reason for the space averaging, given below.

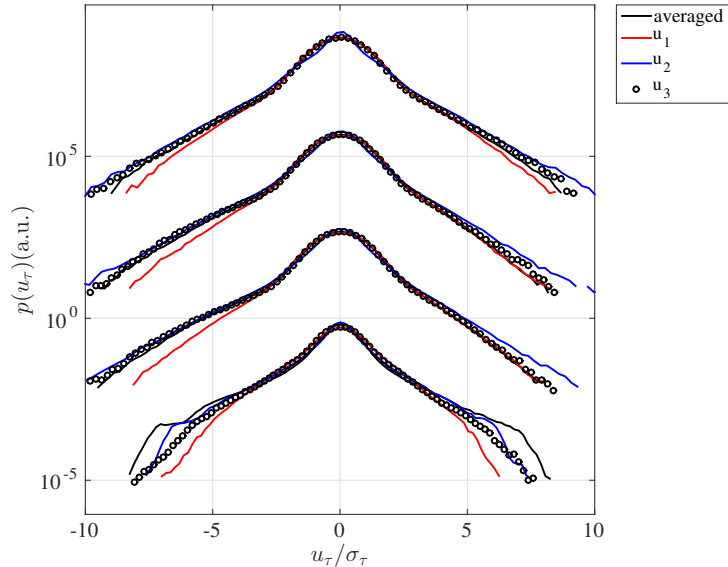


Figure 1: $p(u_\tau)$ for the three single point measurements and the respective space average.

- As described by Reinke et al. [3] in detail, the active grid is made of numerous square metal flaps that are connected by joints equipped with streamlined support structures. Therefore, a single point measurement behind a joint is not as much affected by the movement of the flaps compared to a position behind a flap. Please refer to [3] for details. However, Fig. 1 shows that the intermittent character of the inflow is obvious for all single point measurements as well as the space average. Still, we believe that for inflow characterization a space averaging gives a more appropriate description of the flow affecting the whole rotor.

We clarified this aspect in the revised manuscript as follows:

Following the concept of a rotor effective wind speed used in [2], this approach is more appropriate to describe the wind speed affecting the rotor than a single point measurement. It should be noted that our results are hardly effected by using averaged measurements as opposed to data of the central hot wire. The distance...

If this approach is more appropriate, why is it not used in the following part of the study?

For inflow characterization we used space averaged data for reasons mentioned above. When comparing turbine data to wind speed data, single point

hot wire measurements in front of the turbine were used so that *simultaneously* recorded data can be compared. As we mentioned above there is not a big difference between using averaged and non averaged wind speed. There is definitely another aspect, that each hot wire in front of the turbine will create a small perturbation of the inflow, especially when mounting multiple wire in one plane. Thus we prefer to work only with one hot wire for this comparison.

please show PSD for all signals and discuss them.

Please find the PSDs of the remaining three signals in the figures below. The PSD of the power data, Fig. 2 of this reply, clearly shows the mean rotational speed of the turbine, $\langle\omega\rangle \approx 25.2$ Hz, and the harmonics. Also the PSD of the thrust data (Fig. 3 of this reply) shows the rotation frequency along the the harmonics, although not as clearly as for the power data. More striking are the multiple peaks that we associate with the vibrations of the whole setup including the turbine and the support structures with ground mountings. We do not believe that adding all PSDs to the manuscript will improve quality and readability. We showed the PSD of the hot wire data because the filtered signal is the basis of the approach described in section 3.2. An explanation of the regular drops of the torque-PSD is given in the following aspect.

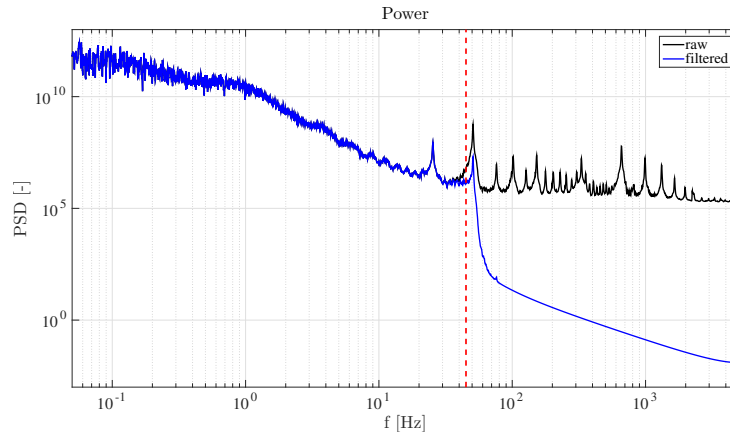


Figure 2: Power spectral density (PSD) of the intermittent power time series, raw (black) and filtered (blue).

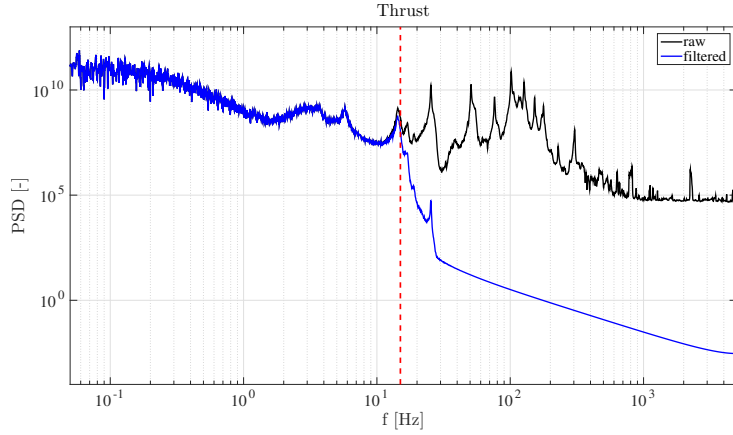


Figure 3: PSD for thrust data.

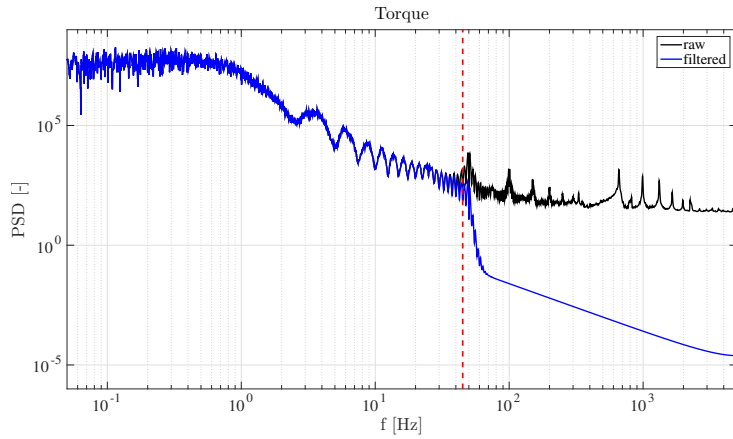


Figure 4: PSD for torque data.

Fig 5 : the coherence functions for power and torque are not continuous, but show regular peaks. Why? Don't we expect continuous functions? Please elaborate an explanation.

The coherence function of power and torque show regular drops at multiples of 2.5 Hz. Both the power and torque depend on the electric current in the circuit, please see equations (6) and (8) in the manuscript. The same drops at multiples of 2.5Hz in the PSD can be found in the PSD of the torque data, see Figure 4 and therewith in the current data itself. The reason for this is a moving average function implemented in the control algorithm of the turbine controller. In Figure 5 we show the PSD of the voltage U_{FET} applied to the field effect transistor for controlling the electrical load.

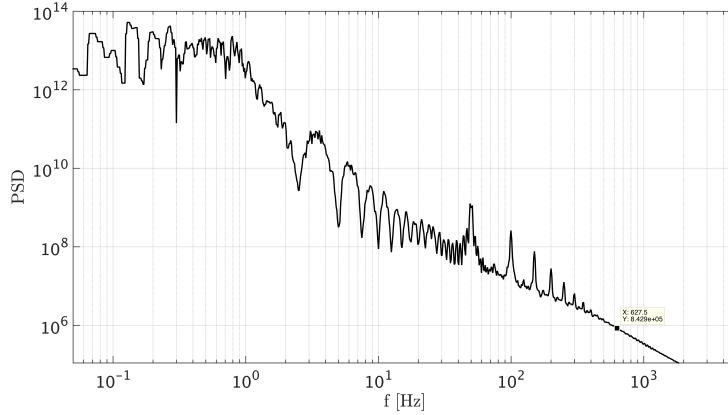


Figure 5: PSD of the voltage signal applied to the field effect transistor, U_{FET} (extract of 1E6 samples).

The update rate of 50Hz shows up in the PSD along with the same drops at multiples of 2.5Hz as in the PSD of the electric current. The tip speed ratio is the controller input, which is smoothed using a moving average filter of 20 samples before being passed to a PI controller within the 50Hz control loop, resulting in the regular drops at multiples of $50\text{Hz}/20 = 2.5\text{Hz}$. To further show, Figure 6 shows the PSD of laboratory turbulence data (hot wire data, sampled at 8kHz) used in [4]. The raw data (black) and the same data set smoothed by a 100 samples moving average filter (red) are shown. As can be seen, periodic drops at multiples $8000\text{Hz}/100 = 80\text{Hz}$ in the PSD are the result of the moving average filter. Due to the definition of the magnitude coherence squared (eq. 10 in the manuscript, see [5] for details.), the drops in the PSD are found in the coherence as well.

It should be stressed that this is a pure signal problem but does not change in principle our findings of this paper. To clarify this point we added the following explanation to the caption of Fig. 5 of the manuscript:

Magnitude-squared coherence of filtered hot wire data and thrust (a) as well as power and torque (b) respectively. 500 Hanning windows with 50 % overlap were used here, as suggested by [5]. Graph (b) shows regular drops of γ^2 which are caused by a filter function within the control algorithm of the model turbine. As the controller affects the electric circuit, there is a direct connects to the electric current and therewith to the power and torque. Consequently, the effect of the filter is clearly visible in this graph.

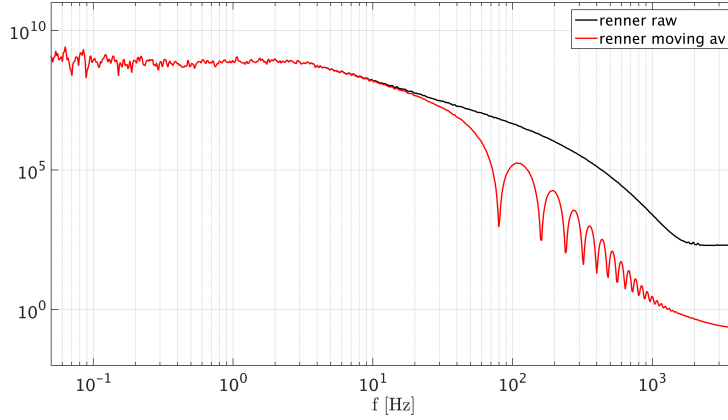


Figure 6: PSD of laboratory turbulence data used in [4] based on raw (black) and smoothed (red) hot wire data.

Wind turbine data sets are low-pass filtered with a cut-off frequency of 15Hz for thrust and 45Hz for power and torque data. These cut-off frequencies are very close to the frequencies related to the time scales of interest, 13 and 40Hz. One can therefore expect that the signal distortion due to filtering (magnitude damping and phase shift) affects the wind turbine signals at the frequencies of interest, and so their unsteady properties, including intermittency. In other words, how confident can one be in the increment PDFs obtained for the thrust with $\tau = 0.067s$, whereas the signal is lowpass filtered at 15Hz; and for the power and torque with $\tau = 0.025s$, whereas the signals are low-pass filtered at 45Hz?

The reason for filtering the data is the presence of noise disturbances as described in Section 3.2. Therefore, the data is not really suitable for testing the effect of shifting the filter frequency and/or the time scale analyzed since it is not possible to distinguish the effect of the filter from the effect resulting from the noise. Because of that we use laboratory turbulence used by Renner et al. [4]. Figure 7 shows the PSD, which does not show any noise peaks which allows us do isolate the effect of low pass filters on the increment PDF.

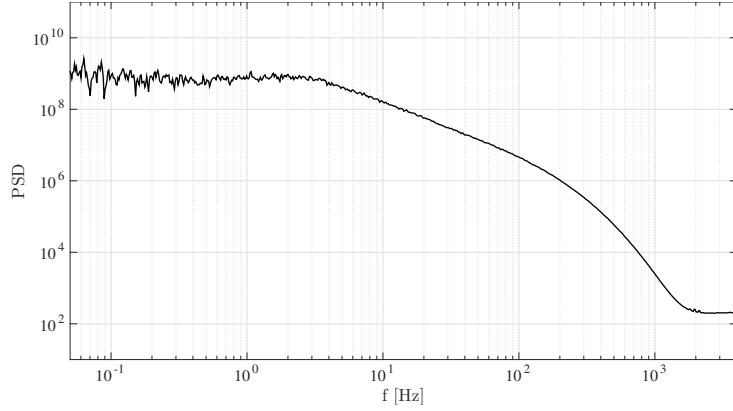


Figure 7: PSD for the lab data used in [4].

We fix the time scale to $\tau = 0.01$ s, which corresponds to a frequency of 100 Hz. We use the same 6th order butterworth low pass filter as in our study to filter the turbulence data exactly at 100Hz (corresponding to the time scale τ) as well as at larger (120Hz) and smaller frequencies (80Hz). Figure 8 shows the increment PDF for the raw data and the filtered version. The same approach is carried out for filter frequencies closer to 100Hz, being 98Hz and 102 Hz, please see Figure 9.

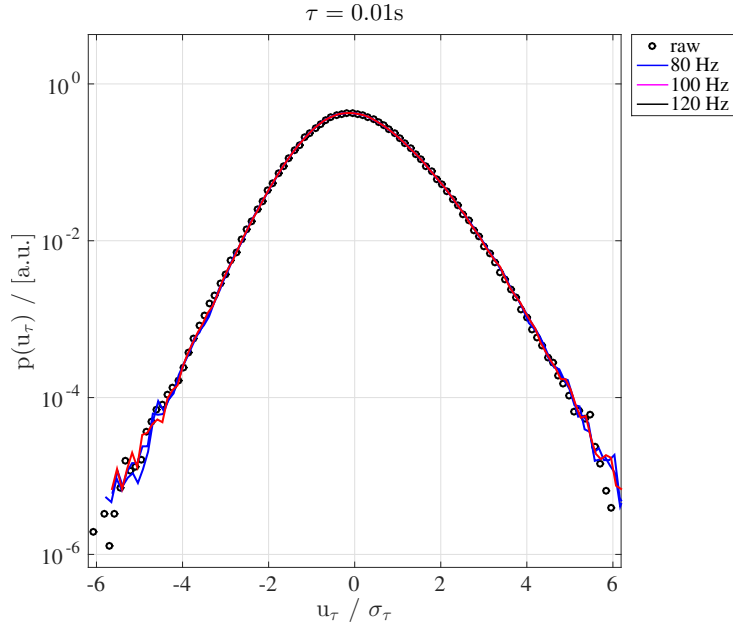


Figure 8: Fixed $\tau = 0.01$ s, butterworth low pass filter at the frequencies shown in legend.

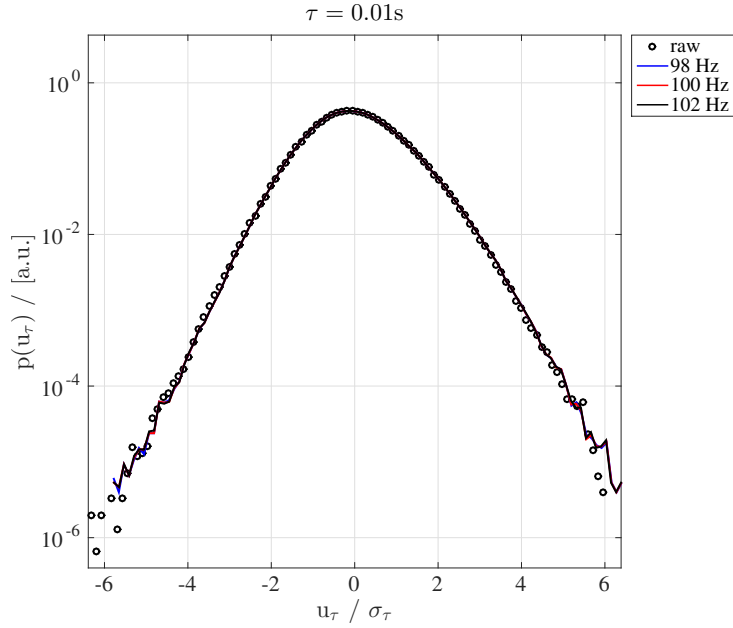


Figure 9: Fixed $\tau = 0.01\text{ s}$, butterworth low pass filter at the frequencies shown in legend.

Herewith we show that the low pass filter does not change the shape of the increment PDF of the lab turbulence. As the magnitude is damped by the filter in frequency space and we consider distributions *normalized* to the standard deviation of the increment time series (cf. Section 2 of the manuscript), the shape of the distribution is not significantly affected.

To clarify, we added the following text to the revised manuscript (p. 17. lines 12 ff.):

...a cutoff frequency of 15Hz was chosen in order to include a scale between the rotor diameter and the blade length. From the analysis of other intermittent data, it can be shown that our filtering used here is not effecting the intermittency effects in an significant way. Thus, the filtering only suppresses noise effects.

Minor comments:

if I compute the frequency related to the time scale 0.08s, I obtain 12 instead of 13Hz.

1/0.08 s = 12.5 Hz. This will be corrected in the updated manuscript.

Fig. 11: use solid lines for the inflow for both plots.

When showing increment PDF throughout this paper, lines were used for wind speed data and symbols for turbine data. To distinguish between Gaussian and intermittent wind speed data, solid lines were used for intermittent and dashed lines for Gaussian data as in p5, Fig.1, p13, Fig.9, p14, Fig.10. Therefore, we would rather not change the line style in Fig.11 for consistency, although Fig. 11(a) shows only one type of inflow. We think that the shape of the distribution is clearly visible.

We agree with all other minor comments and will correct them in the updated manuscript.

References

- [1] Soltani, M. N., Knudsen, T., Svenstrup, M., Wisniewski, R., Brath, P., Ortega, R., and Johnson, K., “Estimation of rotor effective wind speed: A comparison,” *IEEE Transactions on Control Systems Technology*, Vol. 21, No. 4, 2013, pp. 1155–1167.
- [2] Schlipf, D., Schlipf, D. J., and Kühn, M., “Nonlinear model predictive control of wind turbines using LIDAR,” *Wind Energy*, Vol. 16, No. 7, oct 2013, pp. 1107–1129.
- [3] Reinke, N., Homeyer, T., Hölling, M., and Peinke, J., “Flow Modulation by an Active Grid,” *Experiments in Fluids*, 2016, submitted.
- [4] Renner, C., Peinke, J., and Friedrich, R., “Experimental indications for Markov properties of small-scale turbulence,” *Journal of Fluid Mechanics*, Vol. 433, 2001, pp. 383–409.
- [5] Carter, G. C., Knapp, C. H., and Nuttall, A. H., “Estimation of the Magnitude-Squared Coherence Function Via Overlapped Fast Fourier Transform Processing,” *IEEE Transactions on Audio and Electroacoustics*, Vol. 21, No. 4, 1973, pp. 337–344.

Authors' response to Anonymous Referee #2:

We, the authors, are very thankful for the detailed and constructive comments and greatly appreciate the willingness to review our manuscript. Please find our responses below. The original comments are shown in **bold** and the respective answers below. Excerpts of the manuscript are shown in *italic writing*, whereas additions are written in blue and deleted parts in red. Thank you very much.

Specific comments:

1. **You should not have footnotes in Abstract. Abstract should be a stand-alone section without references to the rest of the paper.**

This will be corrected by placing the description of intermittency in section 1.

2. **P1, L11. "The dynamic wind interacts: : :"** What is a dynamic wind? This might imply that there is a static wind, which I never heard of. Wind is movement of air, thus it is dynamic by definition. Why not saying "Wind interacts: : :"

What was meant is that the wind speed is not static. We want to stress here that the wind, which interacts with the turbine, contains fluctuations/turbulence. We changed the text accordingly:

The ~~dynamic~~ turbulent wind interacts with the system dynamics, resulting in the output parameters of a wind energy converter system such as power, mechanical loads or other quantities of interest.

3. **Not sure what is your rule to italicize words. I have nothing against italicizing the important words and terms, but in your manuscript you are using it for that purpose, as well as for the names of some instruments, modules, etc. I suggest you use it only to highlight important words.**

This will be corrected in the updated manuscript and initialization will be limited to important words and phrases.

4. **Citations in the text should be from oldest to the latest. For example, P1, L1 has citations that are in a random order; similarly citations at the end of P1 are also randomly listed. Please correct that throughout the text.**

This will be corrected in the updated manuscript.

5. P1, L20. When discuss the non-Gaussian characteristics of wind, you should mention some of the atmospheric phenomena that create those winds; like downbursts, for example, which are quite frequent in Europe and elsewhere. Gust fronts are other phenomena associated with non-Gaussian winds. There are several papers by Giovanni Solari and his group on that subject. For instance, De Gaetano et al. (2014) demonstrated the non-Gaussianity statistics of some non-synoptic winds (see Figures 2, 3 and 4 in their paper). Papers like this would strengthen your study, as they show that there are some atmospheric phenomena that generate non-Gaussian wind statistics. De Gaetano P, Repetto MP, Repetto T, Solari G. 2014. Separation and classification of extreme wind events from anemometric records. *Journal of Wind Engineering and Industrial Aerodynamics* 126: 132–143. DOI: 10.1016/j.jweia.2014.01.006.

We thankfully notice the mentioned paper and like to include it in the introduction. At the same time, a clearer separation between the analyses of velocity *values* and velocity *increments* seems necessary in the manuscript. Therefore, the introduction was updated and we hope to clearly separate the velocity values and the corresponding statistics from increments, which is the focus of this paper. Increments characterize changes of the wind speed in a given time horizon, which is for example important for loads and the control system acting on actual wind values. Please find the updated version of the introduction at the end of this reply.

6. Symbols in your equations are not the same as symbols in the text. Your $u'(t)$ in the text does not look like $u'(t)$ in equations. It is not italicized in the text. Please be consistent and correct these. (I gave an example of $u'(t)$, but this holds for all of your symbols).

There are indeed discrepancies, which will be corrected in the updated manuscript.

7. What is the reason behind using the wind speed interval between 7 m/s and 8 m/s and not some other or perhaps wider interval?

We chose the interval $7 \text{ m s}^{-1} \leq \langle u(t) \rangle_{10\text{min}} \leq 8 \text{ m s}^{-1}$ because typically a wind turbine is in a very stable operation in partial load conditions

during those wind speeds. We wanted to exclude wind speeds close to cut-in as well as rated power. The interval gave us more than 22×10^6 data point considering 1 year of offshore data, which is more than enough. Regarding our analysis of increment PDFs, wider intervals gave very comparable results as shown in Figure 1 of this reply. Further, it has been shown in [1], Fig.5 that such a constraint will filter out intermittency effects caused by instationary conditions on large scales and thus enables to study more properly small scale turbulence effects. Therefore, we would like to stick to the original [7,8]m/s interval as the mean value and turbulence intensity match our TurbSim simulations. This aspect is further discussed in the following remark 8).

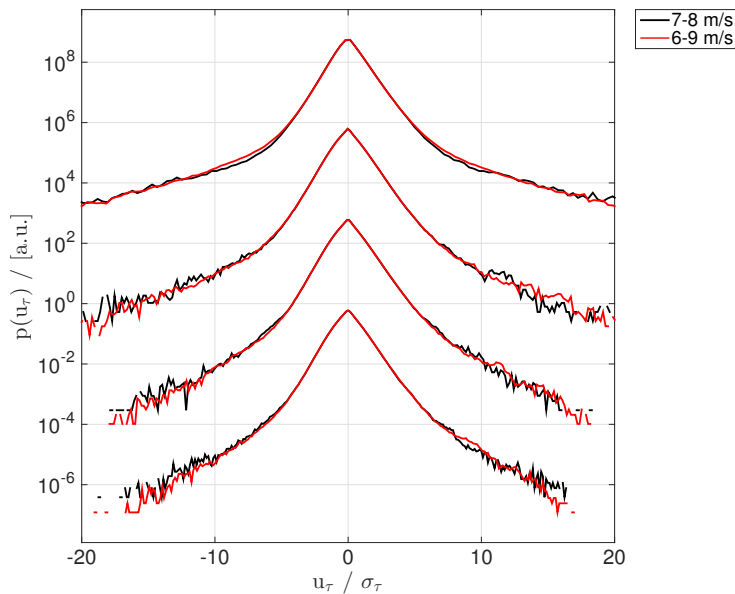


Figure 1: $p(u_\tau)$ for FINO1 data based on different 10min-mean intervals.

To clarify this, we added to the manuscript (p.4, lines 1 ff.):

10Hz data of one year were considered and ten minute records of $7 \text{ m s}^{-1} \leq \langle u(t) \rangle_{10\text{min}} \leq 8 \text{ m s}^{-1}$ were selected. The approximately 3700 records were then combined and used in this analysis, in order to ensure close-to stationary conditions. It has been shown by Morales et al. [1] that such a constraint will filter out intermittency effects caused by instationary conditions on large scales and thus enables to study more properly small scale turbulence effects. It should be noted that only the mean value of one ten minute record is within $7.5 \pm 0.5 \text{ m s}^{-1}$. During

this time span, samples outside of this interval are included. Tab. 1 shows...

8. **You jumped right away to advanced statistical techniques, i.e. structure functions without showing some basic statistics. Please plot wind speed histogram of field measurements and fit it with Gaussian distribution. Synoptic winds show high degree of Gaussianity (please see the reference I provided above and some of the papers cited in that reference). Therefore, it is strange that your filed data are highly non-Gaussian. Thus, I would like to see a histogram and PDF of field measurements. It will also demonstrate that, while wind speed distribution is (maybe) Gaussian, the wind speed increment does not have to be Gaussian. I believe that further contributes to your paper.**

This is a well known feature of stationary turbulence, u' is close a Gauss, whereas increment statistics increasingly deviate from Gaussianity [2], see also Morales et al. [1] for offshore wind data. We added such a statement in the revised paper to make this point clearer to the reader, p.3, lines 13 ff ¹:

Going one step further in the sense of two point quantities, we will consider velocity changes during a time lag τ and refer to them as velocity increments,

$$u_\tau = u(t + \tau) - u(t) \quad (1)$$

throughout this paper. It is important to distinguish between a statistical description of the fluctuations and the increments. In stationary turbulence, $u'(t)$ is close to a Gaussian distribution, whereas increment statistics increasingly deviate from Gauss [2], which is also shown by [1] for offshore data. The n^{th} order moments...

It is shown in the mentioned paper that the intermittency in one-point statistics is caused by the non-stationarity of $\langle u \rangle_T$ and σ_T . Mathematically, this can be shown as done below

$$p(u) = \int p(u|\langle u \rangle_T) \cdot p(\langle u \rangle_T) d\langle u \rangle_T. \quad (2)$$

While $p(u|\langle u \rangle_T)$ might be Gaussian, the term $p(\langle u \rangle_T)$ reveals the large

¹The citation style in the revised manuscript will be consistent, e.g. (Frisch 1995)

scale instationarities and causes the non-Gaussian distribution of $p(u)$. We believe that the introduction of the manuscript should clearly state the difference in analyzing the wind speed (fluctuations) and the increments. Therefore, we changed the introduction to clarify, please find the revised version at the end of this reply. It should be clear now that only velocity increments are analyzed in our paper.

In Section 2 we focused on methods used in our analyses along with relations we found necessary to follow those approaches. As mentioned in the beginning of Sec.2, we purposely did not give a complete overview of methods to describe wind speed time series. Morales et al. [1] give a detailed description of statistical methods that are used to characterize offshore data exemplary. Therefore, we limit the description in Sec. 2 to the aspect used in our analyses (increment distributions) with referring the reader to Morales et al. for further details. In addition to the new introduction, we clarified this aspect in Sec. 2 as follows p. 3, lines 1 ff.:

In this section, we give a brief overview of the methods used in the industry standard and beyond, along with their mathematical background, without claims of completeness. Further, the methods of data analysis used in this study are introduced. We refer to Morales et al. for a more detailed elaboration. A general first step...

9. **Table 1 cuts a sentence in half. Please organize the text so that you don't have these discontinuities. It decreases the readability of your manuscript.**

We will correct this issue before uploading the new manuscript, however, I think a final placement of figures and tables is still to be done due to the two-column layout of the journal publications.

10. **P2, L78. If I am correct, you are using only the interval [7, 8] m/s. That being said, what extreme events are you referring to when you say extreme events are not reflected correctly using standard model.**

We are using the interval $7 \text{ m s}^{-1} \leq \langle u(t) \rangle_{10\text{min}} \leq 8 \text{ m s}^{-1}$, so the mean wind speed of a 10-minute block is in the interval [7,8]m/s. As shown in Figure 1 of the manuscript, we are analyzing time scales of $\tau \leq 60\text{s}$, which are relevant for the turbine dynamics. So by extreme events we are referring to extreme velocity increments of multiple standard deviations σ_τ on small time scales below one minute *within* a 10 minute block of $7 \text{ m s}^{-1} \leq \langle u(t) \rangle_{10\text{min}} \leq 8 \text{ m s}^{-1}$. We changed the manuscript accordingly, p.4, ll 7,8:

As shown in Tab. 1 and Fig. 1, certain characteristics of a wind speed time series, extreme *events velocity increments* in particular, are not reflected correctly using standard methods. In this paper,...

11. **P6, L1.** Why is this spatially averaged wind speed more appropriate to describe the wind speed conditions than a single point measurements? Please explain.

Please refer to our responses to the first referee's comments as this issue is addressed there.

12. **P6, L910.** This sentence has too many semi-colons. Please reformulate this sentence in order to remove these unnecessary semi-colons.

We reformulated this sentence to:

The vacuum-casted rotor blades are based on a SD7003 airfoil profile. Further details on the turbine design are described by [...]. For details about the blade design, see [...].

13. **P6, L27.** Why did you decide to use only a single hot wire signal for the comparison in Section 4.2 and not the spatially averaged data that you used for flow characterization?

Please refer to our responses to the first referee's comments as this issue is addressed there.

14. **What are the uncertainties and errors in all your measurements (wind tunnel, field measurements, thrust, etc.)? Uncertainties in measurements should be well documented.**

The offshore data is publicly available and uncertainties are well documented. For the respective anemometer, which was used in our study, the uncertainty is $\approx 3\%$ [3]. We suggest to add this information along with the respective citation to the manuscript.

For the experimental data, we estimate the statistical error of the increment PDFs by $err \approx 1/\sqrt{n}$, where n is the number of events in each bin of the respective increment. For better judgment of the statistical significant of extreme events, we mark every bin with an error $< 10\%$ ($n < 100$) with a red \times as exemplary done for Fig. 11(b) of the manuscript below:

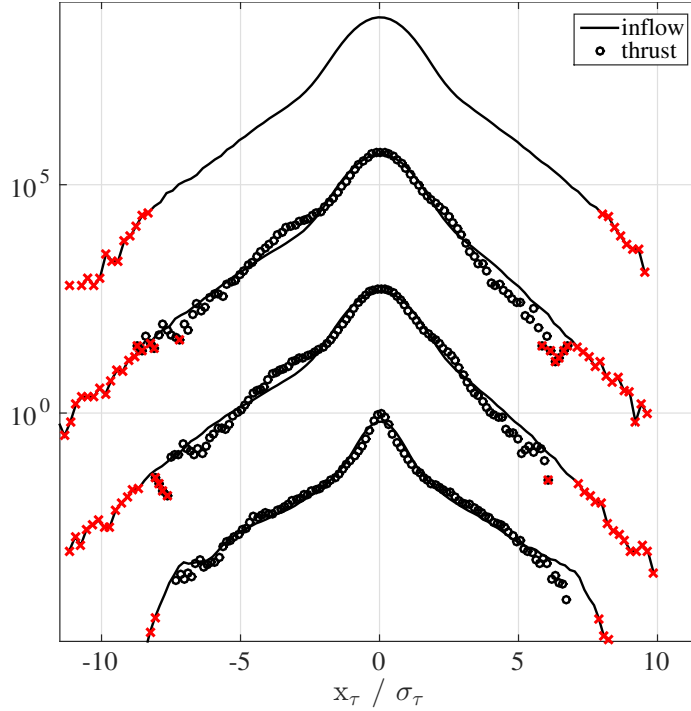


Figure 2: Increment PDF of inflow and thrust data. Data point with an estimated error exceeding 10 % are marked in red.

We suggest to describe this procedure and to mask values with a statistical error exceeding 10% for every increment-PDF shown in the updated manuscript,.

15. **In Figure 6, is the time series of wind speed synthetically created or is it from the wind tunnel measurements (or maybe field measurement)? Either way, that time series looks very artificial to me. Also, you said that your field measurements are in the interval [7, 8] m/s, but your wind speeds in Figure 6 are around 5 m/s. Is it due to the scaling or something else? Please explain.**

The wind speed time series shown in Figure 6 is based on hot wire measurements upstream of the turbine during the intermittent inflow created by the active grid, which will be formulated more clearly in the updated version of the manuscript p.9, lines 3 ff:

Fig. 6 shows examples of the time series of the four different signals, filtered and unfiltered. The graph in Fig. 6(a) shows the wind speed during the intermittent inflow upstream of the turbine. The other

graphs show the simultaneously recorded signals of the turbine.

Due to the blockage of the turbine, the wind speed shown in this figure is smaller than 7m/s, which is the approximate wind speed at the rotor's position *without* the turbine being installed, please see section 4.1.

16. **P10, L6. What is the purpose to analyze scales that cannot be produced in your wind tunnel? That length scale cannot be replicated inside of your chamber.**

The largest *time* scale we analyze is $\tau = 2$ s. Applying Taylor's hypothesis gives a length scale of 14 m, which is larger than the test section. However, Taylor's hypothesis gives an idea of the length scale corresponding to a time scale τ . This does not mean that such a large structure is present in the test section at one point of time. Further, Knebel et al. [4] show experimentally that velocity time series with an integral length scale larger than the grid itself can be created in the wind tunnel with the active grid. We do think that it makes sense to analyze a time scale of $\tau = 2$ s. We reformulate the manuscript at p.10, lines. 6 ff:

The largest scale considered is $\tau = 2$ s, ~~which corresponds to approximately 14 m and is thus larger than the test section of the wind tunnel.~~ Thus, the turbine experiences a flow situation corresponding to a 14 m structure in the wind field having an impact on the model turbine.

The interpretation of a 14-m structure being present at one time in the wind tunnel is misleading, although velocity changes in the range of seconds can be created. The reformulated section should clarify this.

17. **Your Table 2 is very confusing. What does the number 0.067 represent? That is, what is the column between “rotor diameter” and “order of blade length”?**

In the original Table 2, each column corresponds to one of the four time scales τ considered in the increment analysis. The number 0.067 represents the time scale of $\tau = 67$ ms. We suggest to update the table for better clarity, please find it below.

	scale 1	scale 2	scale 3	scale 4
time scale τ [s]	2	0.08	0.067	0.025
length/D [-]	≈ 24	1	≈ 0.8	0.3
physical object *	-	rotor diameter	-	order of blade length

Table 1: Overview of scales considered in relation to certain characteristic turbine lengths. The time scales τ were used in the analysis. To get an idea of the spatial dimension, Taylor’s hypothesis is used to transfer from time to space with $\langle u \rangle \approx 7 \text{ m s}^{-1}$. The obtained length scale is expressed as multiples of the rotor diameter for better comparison. The length is further related to physical objects of the turbine to get a sense of the dimensions.

*) The physical object relates the length scales based on Taylor’s hypothesis to dimensions of the model wind turbine.

18. **P11, L3. “: : : analysis, two different, purposely created: : :”**
Please reformulate this sentence. Sounds strange.

We suggest to reformulate this sentence to:

Throughout the following analysis, two different, ~~purposely created~~ flow situations will be considered and used as inflow conditions for the model wind turbine.

19. **P17, L15. Vortex shedding, i.e. frequencies at which vortex shed is defined by the Strouhal number, which in turn depends on the Reynolds number. That being said, how is that shedding does not depend on fluctuations in inflow? Please elaborate. If needed, please take a look at Zdravkovich’s books on flow around circular cylinders.**

As mentioned, the shedding frequency is defined by the Strouhal number. The shedding also occurs during laminar inflow and does therefore not depend on the fluctuations in the inflow.

The purpose of this example is to show that an object in the flow might experience dynamics/fluctuations that do not result from velocity fluctuations in the inflow. Such effects might occur in the experiments, however, we try to focus on the turbine dynamics that *do* result from the inflow turbulence. As this example might cause more confusion than adding completeness, we suggest to delete the specific example and reformulate as follows:

*Also, there might be aerodynamic effects that are of even higher frequency than the inflow fluctuations, and **are** therefore not captured due*

to the filtering. ~~As a straightforward example, a laminar flow passing a cylinder results in a well-defined frequency due to von Kármán vortex shedding, cf.[...]. The shedding does result from the inflow, although not being related to the fluctuations. Thus, aerodynamic...~~ Such effects at the rotor are possibly excluded by the low frequency filtering. This study, however, focuses on dynamics caused by the inflow turbulence.

20. **P17, L16. Based on the circular cylinder example, how did you conclude that some aerodynamic effects might be excluded due to low frequency filtering? You use a “Thus” at the beginning of that sentence and I do not see how that claim results from the previous discussion. Please explain.**

As mentioned in the previous comment, we mention effects of higher frequency than the inflow fluctuations. This implies that those frequencies are larger than the cutoff frequency of the low pass filter, cf. Fig. 5 in the manuscript. However, as this example will be deleted as mentioned in the previous comment, we do not think that a more detailed description is needed in the manuscript.

21. **The last sentence in the Discussion section is confusing. To me, it sounds like you are saying that the focus of this study is to analyze what is presented in the study, which is redundant. Please reformulate or explain what information you want to convey in that sentence.**

The last paragraph of the discussion states that we do not claim full scalability due to the mentioned reasons. We agree that the last sentence does not really fit in here as mentioning the main findings should be done in the conclusion. We delete the last sentence of the discussion.

22. **I believe you should emphasize more on the importance of your study in the Discussion section. Try to relate your findings, at least qualitatively, with the real atmospheric conditions. Also, what would be the application of your study? When can we expect non-Gaussian velocity increments and when are they Gaussian in real atmosphere? Moreover, are they ever Gaussian? All these questions could be addressed in Introduction and/or Discussion. Providing answers to those and similar questions would greatly improve the readability and contributions of your paper.**

In this study we focus on time scales $\tau \leq 60$ s regarding atmospheric data. We show in Fig. 1 that those increment PDF are far from Gaussian as also shown in the cited works. Throughout this paper, we concentrate on the discrepancy between the intermittency of the data and the Gaussian assumption by the industry standards. The application is to show whether this discrepancy is relevant for wind turbines. This is stated in the conclusion. However, we agree that this should be stated more clearly. We will add to the introduction p.2, line 19.:

It is not clear to what extent non-Gaussian flow conditions transfer to turbine data. At the same time, this is a very important aspect in the design process of wind turbines and in the wind field models used. Wrong assumptions of the conversion from turbulence characteristics to wind turbine data might lead to faulty dimensioning and problems in the integration of wind energy in the power grid.

23. **P18, L1. “Our results show: : :” Please reformulate this sentence. Not clear what you want to say.**

What was meant is that the intermittency in the inflow is not filtered by the turbine so that the turbine data is intermittent in a similar way. We reformulate the sentence as follows:

Our results ~~show no~~ do not show any filtering of the intermittent features of wind speed fluctuations found in real wind fields by the turbine. Consequently one should be aware that wind characteristics, which are not reflected in standard wind field descriptions, e.g. the IEC 61400-1, have a significant impact on wind turbines.

24. **Lastly, I advise the authors to find a native English speaker to proofread the manuscript.**

The updated manuscript will be carefully proofread.

References

- [1] Morales, A., Wächter, M., and Peinke, J., “Characterization of wind turbulence by higher-order statistics,” Wind Energy, Vol. 15, No. 3, 2012, pp. 391–406.
- [2] Frisch, U., Turbulence : the legacy of A.N. Kolmogorov, Vol. 1, Cambridge university press, 1995.
- [3] Westerhellweg, A., Neumann, T., and Riedel, V., “Fino1 mast correction,” Dewi magazin, Vol. 40, 2012, pp. 3.

- [4] Knebel, P., Kittel, A., and Peinke, J., “Atmospheric wind field conditions generated by active grids,” Experiments in Fluids, Vol. 51, No. 2, 2011, pp. 471–481.

On the impact of non-Gaussian wind statistics on wind turbines - an experimental approach

Jannik Schottler¹, Nico Reinke¹, Agnieszka Hölling¹, Jonathan Whale², Joachim Peinke¹, and Michael Hölling¹

¹ForWind, University of Oldenburg, Institute of Physics, Küpkersweg 70, 26129 Oldenburg, Germany

²Murdoch University, School of Engineering and Information Technology, Murdoch, WA, 6150 Australia

Correspondence to: Jannik Schottler (jannik.schottler@forwind.de)

Abstract. The effect of intermittent ¹ and Gaussian inflow conditions on wind energy converters is studied experimentally. Two different flow situations were created in a wind tunnel using an active grid. Both flows exhibit nearly equal mean velocity values and turbulence intensities, but strongly differ in their two point statistics, namely their distribution of velocity increments on a variety of time scales, one being Gaussian distributed, the other one being strongly intermittent. A horizontal axis model wind turbine is exposed to both flows, isolating the effect of the differences not captured by mean values and turbulence intensities on the turbine. Thrust, torque and power data were recorded and analyzed, showing that the model turbine does not smooth out intermittency. Intermittent inflow is converted to similarly intermittent turbine data on all scales considered, reaching down to sub-rotor scales in space, indicating that it is not correct to assume a smoothing of [wind speed fluctuations](#) [intermittent wind speed increments](#) below the size of the rotor.

10 1 Introduction

Wind energy converters (WECs) work in a turbulent environment and are therefore turbulence driven systems. The [dynamic turbulent](#) wind interacts with the *system dynamics*, resulting in the output parameters of a wind energy converter system such as power, mechanical loads or other quantities of interest.

Generally, the characteristics of the output dynamics of a WEC need to be understood in detail for multiple reasons. Power fluctuations have been reported in numerous studies, causing challenges in grid stability

~~(e.g. Chen and Spooner, 2001; Sørensen et al., 2007; Carrasco et al., 2006)~~

[\(e.g. Chen and Spooner, 2001; Carrasco et al., 2006; Sørensen et al., 2007\)](#). Drive train and gearbox failure rates remain high, adding to the cost of energy since gearboxes are among the most expensive parts of WECs. These types of failures are likely to be linked to torque fluctuations (e.g. Musial et al., 2007; Feng et al., 2013). Next, turbulent wind affects extreme and fatigue loads, which is clearly related to the lifetime of WECs (Burton et al., 2001).

Wind dynamics in the atmospheric boundary layer have been investigated extensively. [Here, one has to differentiate between analyses concerning the statistics of the wind speed values and velocity increments. The wind velocities might become](#)

¹It should be noted that, throughout this paper, *intermittency* refers to a non-Gaussian, heavy-tailed distribution of *increments* as defined in Sec. 2.

anomalously distributed due to large scale meteorological events like downbursts or thunderstorms (De Gaetano et al., 2014). Velocity increments, on the other hand, characterize statistically the temporal aspect of fluctuations, whose non-Gaussian statistics are well-known from small scale turbulence (Frisch, 1995). Active systems, like wind turbines as discussed here, adapt to actual wind situations, thus we focus in this contribution on wind speed changes within seconds, i.e. by the corresponding

5 increments. Numerous studies report on non-Gaussian characteristics of wind speed ~~fluctuations, see (e.g. Boettcher et al., 2003; Morales et al., 2012; Wächter et al., 2012; Liu et al., 2010)-~~ increments, see (e.g. Boettcher et al., 2003; Liu et al., 2010; Morales et al., 2012; Wächter et al., 2012). Further, findings of non-Gaussian wind statistics have been implemented in simulations by a variety of methods, see (e.g. Nielsen et al., 2007; Gong and Chen, 2014; Mücke et al., 2011)-

10 (e.g. Nielsen et al., 2007; Mücke et al., 2011; Gong and Chen, 2014).

In the field of wind energy research, it is still unclear to what extent wind dynamics transfer to the parameters of a WEC such as loads, power etc. Most likely, this depends on the relevant time scales, which change with the system dynamics. Therewith, the conversion from wind to power, loads etc. vary with the turbine type. Consequently, it is of importance what scales in time and space are relevant to quantify the impact of turbulent wind on WECs (van Kuik et al., 2016) and scale dependent analyses

15 become necessary.

Mücke et al. (2011) found that intermittent inflow conditions do not affect rain flow distributions of the torque significantly. However, similarly intermittent torque ~~fluctuations-increments~~ based on a numeric wind turbine model used in ~~FAST-the~~ FAST (Jonkman and Buhl Jr, 2005) in combination with AeroDyn (Moriarty and Hansen, 2005) were found. Gong and Chen (2014) investigated the short and long term extreme response distributions of a wind turbine during Gaussian

20 and non-Gaussian inflow conditions using ~~the aeroelastic tool FAST (Jonkman and Buhl Jr, 2005)~~ FAST. The extreme turbine responses to non-Gaussian inflow were considerably larger than the ones to Gaussian wind. However, Berg et al. (2016) recently reported a vanishing effect of non-Gaussian turbulence on extreme and fatigue loads based on large-eddy simulation (LES) generated wind fields in combination with aeroelastic load simulations using HAWC2 (Larsen and Hansen, 2007). It was concluded that non-Gaussianity in sub-rotor size eddies ~~are-is~~ filtered by the rotor. In contrast, Milan et al. (2013) showed

25 that, based on field data, multi-MW WECs convert intermittent wind speeds to turbulent like, intermittent power with fluctuations down to the scales of seconds. Even on the scale of an entire wind farm, intermittent power output was reported. To summarize, different simulations and data from real turbines deliver an inconclusive answer on our posed question on the conversion from turbulent inflow to wind turbine data. It is not clear to what extent non-Gaussian flow conditions transfer to turbine ~~data~~ parameters. At the same time, this is a very important aspect in the design process of wind turbines and in the wind

30 field models used. Wrong assumptions of the conversion from turbulence characteristics to turbine data might lead to faulty dimensioning and problems in the integration of wind energy in the power grid.

With the present work we contribute through wind tunnel experiments to the ongoing discussion on the conversion process of non-Gaussian wind statistics to wind turbine data such as power, thrust and torque. A model wind turbine and an active grid for flow manipulation were used in order to examine to what extent Gaussian distributed and highly intermittent wind speeds

35 affect the model turbine dynamics differently.

This paper is organized as follows: Sec. 2 gives an overview of commonly used methods to characterize wind speed time series, parts of which are applied to offshore measurement data and simulated wind speed time series. Mathematical tools used throughout this paper are introduced here. Next, Sec. 3 describes the experimental methods used, including the setup, the definition of examined quantities and their processing. Sec. 4 shows the results of the experiments, which are discussed in Sec. 5. Finally, Sec. 6 gives the conclusion of the findings.

2 Atmospheric flows

As WECs work in turbulent wind conditions, a proper characterization of these conditions becomes necessary (van Kuik et al., 2016). The industry standard IEC 61400-1 defines procedures for wind field description (International Electrotechnical Commission, 2005). Ten minute mean values and turbulence intensities are considered along with power spectral densities. Therewith, only the first two statistical moments of a velocity time series are taken into account.

In this section, we give a brief overview of the methods used in the industry standard and beyond, along with their mathematical background, without claims of completeness. Further, the methods of data analysis used in this study are introduced. We refer to Morales et al. (2012) for a more detailed elaboration.

A general first step to characterize a time series of wind velocities, $u(t)$, is the definition of velocity fluctuations (Burton et al., 2001),

$$u'(t) = u(t) - \langle u \rangle, \quad (1)$$

where $\langle u \rangle$ denotes the mean value of $u(t)$. A commonly used quantification of the general level of turbulence is the turbulence intensity (TI),

$$TI = \frac{\sigma_{\tilde{T}}}{\langle u \rangle_{\tilde{T}}}, \quad (2)$$

with $\sigma_{\tilde{T}}$ being the standard deviation of $u(t)$ during the time \tilde{T} (Burton et al., 2001). Accordingly, $\langle u \rangle_{\tilde{T}}$ denotes the mean value over the same time span, which is typically ten minutes in industry standards. Notice, since $\sqrt{\langle u'^2(t) \rangle_{\tilde{T}}} = \sigma_{\tilde{T}}$ and $\sqrt{\langle u^2(t) \rangle_{\tilde{T}}} = \langle u \rangle_{\tilde{T}}$, only the first two statistical moments of the one point quantity u' are considered when describing a velocity time series by its fluctuations and/or turbulence intensity as previously defined.

Going one step further in the sense of two point quantities, we will consider velocity changes during a time lag τ and refer to them as velocity *increments*,

$$u_{\tau}(t) = u(t + \tau) - u(t) \quad (3)$$

throughout this paper. It is important to distinguish between a statistical description of the fluctuations and the increments. In stationary turbulence, $u'(t)$ is close to a Gaussian distribution, whereas increment statistics increasingly deviate from Gaussianity (Frisch, 1995), which is also shown by Morales et al. (2012) for offshore data. The n^{th} order moments of u_{τ}

$u_\tau(t)$ are commonly referred to as n^{th} order structure functions (Wächter et al., 2012). The second order structure function,

$$\langle u_\tau(t)^2 \rangle = \langle (u(t+\tau) - u(t))^2 \rangle, \quad (4)$$

is directly linked to the autocorrelation function $R_{uu}(\tau)$, see (Morales et al., 2012) for details $R_{uu}(\tau)$.

$$\langle u_\tau(t)^2 \rangle = 2\langle u(t)^2 \rangle - 2\langle u(t)u(t+\tau) \rangle \quad (5)$$

$$= 2\langle u(t)^2 \rangle (1 - R_{uu}(\tau)), \quad (6)$$

with the assumption that $\langle u(t)^2 \rangle = \langle u(t+\tau)^2 \rangle$. The autocorrelation function of $u'(t)$ and $u'(t+\tau)$.

$$R_{uu}(\tau) = \frac{1}{\sigma_u^2} \langle u(t)u(t+\tau) \rangle, \quad (7)$$

is connected to the power spectral density (PSD) by the Fourier transformation¹. Therewith, the PSD, which is used broadly in wind field models such as the well-known Kaimal model (Kaimal et al., 1972), comprises the same information as the second order structure function.

In order to include all higher order structure functions, $\langle u_\tau^n \rangle$, we will consider the probability density functions (PDF) of velocity increments, $p(u_\tau)$, for different time lags τ and refer to them as *increment PDF*. We normalize u_τ by its standard deviation σ_τ .

$$\sigma_\tau = \sqrt{\frac{1}{N-1} \sum_{i=1}^N (u_{\tau_i} - \langle u_\tau \rangle)^2}, \quad (8)$$

for better visual comparison. The statistical error of each bin of the PDF is estimated by $1/\sqrt{\tilde{n}}$, where \tilde{n} is the number of events in the respective bin. Throughout our analyses, values with a statistical error exceeding 10% are marked with a red \times .

For design load calculations, different turbulence models are used. One, which is suggested by the IEC standard, is the Kaimal model, which considers power spectral densities and features merely Gaussian statistics. In this paper, we investigate to what extent wind characteristics not captured by standard models impact wind turbines. For further instance, we consider a synthetic wind speed time series based on the Kaimal turbulence model, created using the software TurbSim (Jonkman, 2009) and compare it to offshore wind speed measurements, taken from the FINO1 offshore measurement platform at 80 m height. The offshore data set is documented by Westerhellweg et al. (2012). 10 Hz data of one year were considered and ten minute records of $7 \text{ m s}^{-1} \leq \langle u(t) \rangle_{10 \text{ min}} \leq 8 \text{ m s}^{-1}$ were selected. The approximately 3700 records were then combined and used in this analysis, in order to ensure close-to stationary conditions. It has been shown by Morales et al. (2012) that such a constraint will filter out intermittency effects caused by instationary conditions on large scales and thus enables to study more properly small scale turbulence effects. It should be noted that only the mean value of one ten minute block is within $7.5 \pm 0.5 \text{ m s}^{-1}$. During this time span, samples outside of this interval are included. Tab. 1 shows the mean values, standard deviations and turbulence intensities of both data sets. As can be seen, the synthetic time

¹ $\mathcal{F}\{R_{u'u'}(\tau)\} = S(f)$, $\mathcal{F}\{R_{uu}(\tau)\} = S(f)$, with $\sigma_{u'}^2 = \int S(f) df$ and $\sigma_u^2 = \int S(f) df$ and $S(f)$ being the power spectral density (Press et al., 1992).

time series	$\langle u \rangle$ [m s ⁻¹]	σ_u [m s ⁻¹]	TI [%]
Kaimal	7.51	0.54	7.21
FINO1	7.50	0.54	7.18

Table 1. First two statistical moments and turbulence intensities of a synthetic wind speed time series based on the Kaimal model and offshore data (FINO1). Values are rounded to two decimal places.

series and the field measurements are very similar regarding their mean values and turbulence intensities (cf. Tab. 1). Going further, Fig. 1 shows $p(u_\tau)$ of both data sets, showing distinct differences regarding their distributions of increments. The Kaimal model comprised purely Gaussian statistics, while the offshore data feature intermittent increment distributions. As shown in Tab. 1 and Fig. 1, certain characteristics of a wind speed time series, extreme events-velocity increments in partic-

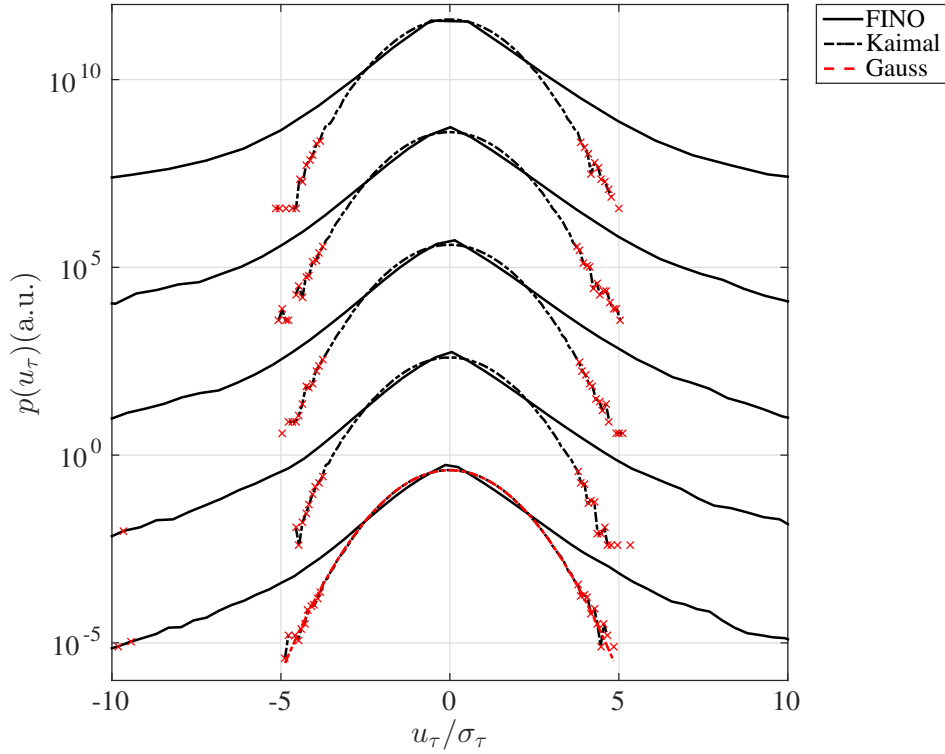


Figure 1. $p(u_\tau)$ for data sets based on the Kaimal model (black dashed line) and for offshore measurements, conditioned so that $\langle u \rangle = 7.5 \pm 0.5 \text{ m s}^{-1}$ (black solid). The PDF for each scale are shifted vertically for better comparison, which is done throughout this paper. Scales from top to bottom $\tau = \{60 \text{ s}, 30 \text{ s}, 10 \text{ s}, 5 \text{ s}, 1 \text{ s}\}$.

ular, are not reflected correctly using standard methods. In this paper, we elaborate if, and to what extent flow characteristics that are *not* captured by the standards (e.g. the first two statistical moments) impact wind turbines. We follow an experimental approach using a model wind turbine in a wind tunnel equipped with an active grid, allowing the generation of various turbu-

lent inflow conditions. By tuning the intermittency while preserving mean wind speeds and turbulence intensities, the effect of intermittency is isolated.

3 Methods

3.1 Experimental setup

5 Wind tunnel and active grid

The experiments were conducted in a wind tunnel of the University of Oldenburg in open jet configuration. The outlet of 0.8 m × 1 m (height × width) was equipped with an active grid for turbulence generation [with a similar design](#) as described by [Reinke et al. \(2016\)](#) [Weitemeyer et al. \(2013\)](#). The grid is made of nine vertical and seven horizontal axes with square metal plates attached. 16 stepper motors allow an individual motion of the axes and thus flow manipulation. However, throughout the experiments, all axes were excited simultaneously. We define a flap angle α , whereas $\alpha = 0^\circ$ [is in alignment](#) with the main flow direction (*open*) and $\pm 90^\circ$ corresponds to maximum blockage, respectively. At $\alpha = 0^\circ$, the blockage of the grid is ~~approx.~~ [approximately](#) 6%, considering the cross sectional area of the grid in relation to the wind tunnel outlet ([Reinke et al., 2016](#)).

The excitation protocols of the motors were designed so that two different flow situations with the same mean wind velocities and comparable turbulence intensities were realized. At the same time, they strongly differ in their distributions of increments: one flow (A) being Gaussian distributed, the other one (B) being highly intermittent on a broad range of time scales, showing a distinctly heavy-tailed distribution of velocity increments. The resulting time series are discussed in Sec. 4.1. The excitation protocol resulting in the intermittent flow features an *active* flow modulation, where α was changed appropriately at a maximal rate of 50 Hz. For the Gaussian flow, the axes were not moved dynamically, so that $\dot{\alpha} = 0^\circ$ [is](#).

The flows considered were characterized using three ~~1D~~ [single-wire](#) hot wire probes simultaneously in one plane normal to the main flow direction. The probes were arranged so that one is located at the position of the model wind turbine's hub ~~, which was installed after flow characterization. The other two probes were positioned and the other two~~ in 0.6 D distance ~~in vertical and horizontal displacement at the same stream-wise position, D = 0.58 m being the rotor diameter of the model turbine displaced in y- and z-direction (cf. Fig. 2). It should be noted that the turbine was not installed during flow characterization.~~ The hot wires are 1.25 mm long with a diameter of 5 μ m. A constant temperature anemometry (CTA) module ([Dantec 9054N0802](#) [Dantec 9054N0802](#)) with a built-in low pass filter set to 5 kHz was used. Data were recorded at 10 kHz for 25 minutes using a [National Instruments cRIO-9074](#) [National Instruments cRIO-9074](#) real time controller with in-house built LabView software. When analyzing the flows, spatially averaged mean values of the three simultaneous measurements,

$$u(t) = \frac{1}{3} \sum_{i=1}^3 u_i(t), \quad (9)$$

are considered, where the index i denotes the respective hot wire. ~~This~~ [Following the concept of a rotor effective wind speed as used by Schlipf et al. \(2013\)](#), [this](#) approach is more appropriate to describe the wind speed affecting the rotor than a single

point measurement. It should be noted that our results are hardly affected by using averaged measurements as opposed to data of the central hot wire. The distance from the active grid to the rotor and hence the hot wires was 1.1 m, which was set as a compromise between two aspects: first, the further away from the outlet, the greater the influence of the emerging shear layer becomes (Mathieu and Scott, 2000), which should be limited; second, the interaction of the rotor's blockage with the active grid increases with smaller distances. Also, the evolution of the turbulence intensity and intermittency was found to decay constantly around 1 m behind the grid (~~?)~~ (Weitemeyer et al., 2013). Consequently, a distance of 1.1 m was chosen to balance the described effects.

Model wind turbine

A three bladed, horizontal axis model wind turbine with a rotor diameter of ~~D=0.58 m~~ D=0.58 m was used. The vacuum-casted rotor blades are based on a SD7003 airfoil profile; ~~further.~~ Further details on the turbine design are described by Schottler et al. (2016); ~~for.~~ For details about the blade design, see (Odemark, 2012). We consider the electrical power,

$$P = P_{el} = U_{gen} \cdot I, \quad (10)$$

where U_{gen} is the generator voltage and I is the electric current of the circuit. I is obtained by measuring the voltage drop U_{sh} across a shunt resistor of $R_{sh} = 0.1 \Omega$, so that Eq. (10) becomes

$$P = U_{gen} \cdot \frac{U_{sh}}{0.1 \Omega}. \quad (11)$$

According to the generator's specifications, the torque T is proportional to the electric current I ,

$$T = k \cdot I \quad (12)$$

with $k = 79.9 \text{ mN A}^{-1}$. The turbine features an automatic load control, with the process variable of the controller being the tip speed ratio (TSR) based on hub height wind speed measurements using a hot wire probe $\frac{2}{3}D$ upstream of the rotor, cf. Fig. 2. The generator's load is controlled using an external voltage applied to a field-effect transistor (FET) within the electric circuit, see (Schottler et al., 2016) for details. Throughout this study, the TSR was set to $\lambda_{set} = 7$, based on $u_{\infty} = 7 \text{ m s}^{-1}$ to ensure a stable point of operation (not in stall) during the experiments.

To measure the thrust force acting on the turbine, it was placed on a three component force balance (ME-Meßsysteme K3D120-50 ME-Meßsysteme K3D120-50 N). Only the thrust force in main flow direction is considered, thus

$$F = F_{thrust, x}. \quad (13)$$

The setup is sketched in Fig. 2; Fig. 3 shows a photograph. As shown in Fig. 2, three hot wires were installed upstream of the rotor during turbine operation. In contrast to the flow characterization, only the center hot wire signal at hub height was used when comparing inflow data to turbine data as done in Sec. 4.2.

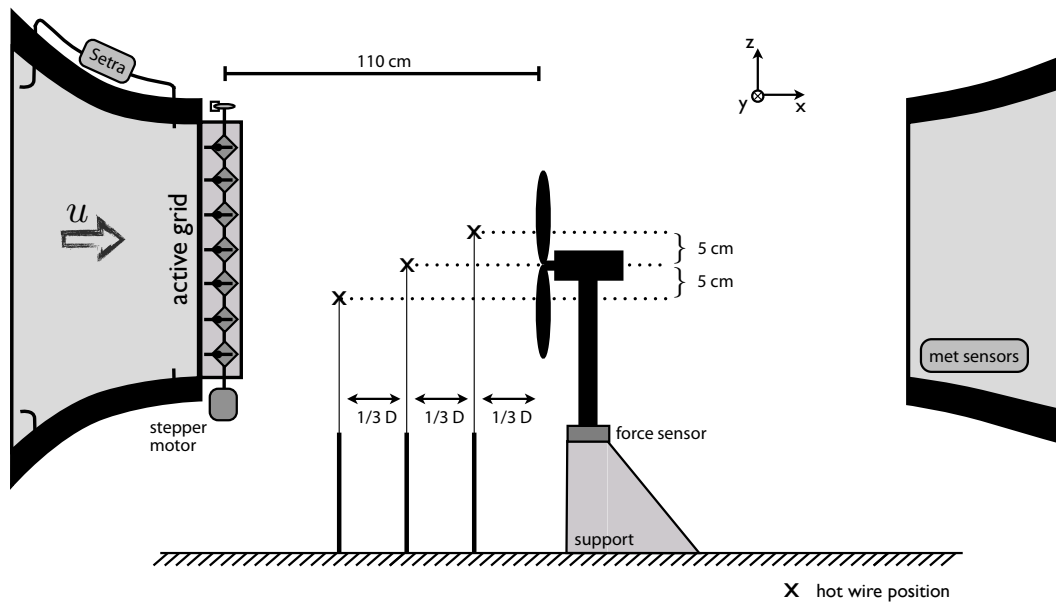


Figure 2. Schematic drawing of the experimental setup, side view. Scales do not match, $D=0.58\text{m}$, $D=0.58\text{m}$.

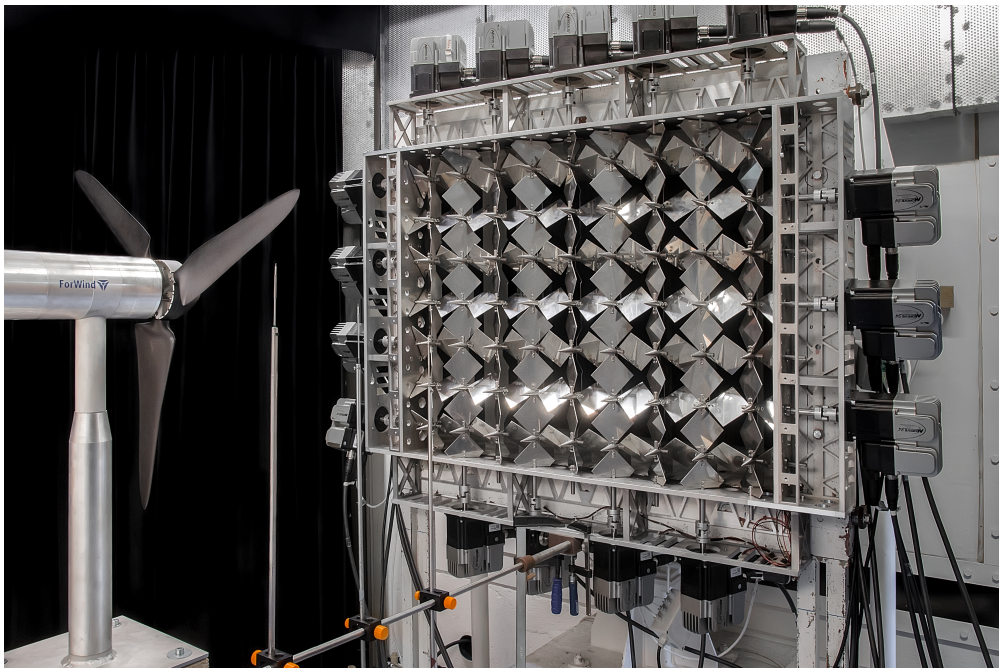


Figure 3. The model wind turbine and the active grid installed in a wind tunnel of the University of Oldenburg.

3.2 Data processing

For each experiment, data were recorded simultaneously. During flow characterization, the three hot wire probes were synchronized and during turbine data acquisition, the thrust force, power, torque and the hot wire signals were recorded synchronously. Generally, all data sets are superimposed with some kind of measurement noise, which we generally want to exclude from our analysis, while preserving the fluctuations of the turbine signals resulting from the inflow. As we analyze different parameters, an appropriate filtering of the different raw signals should, nonetheless, allow a comparison of their statistics. To begin with, $u(t)$ during the intermittent inflow B is filtered using a 6th order Butterworth low pass filter. The cut off frequency is set to 2kHz, since high frequency noise, which is typical for hot wire anemometers (Jørgensen and Hammer, 1999), should be filtered. Further, the resolved length scales corresponding to 2kHz ($\sim 1\text{mm}$) ($\sim 1\text{mm}$), using Taylor's hypothesis (Mathieu and Scott, 2000)) are reasonably small for our purposes. Fig. 4 shows the PSD of the intermittent inflow (B) based on raw and filtered data. As we want to concentrate on the fluctuations of turbine data caused by the inflow, we estimate a maximal

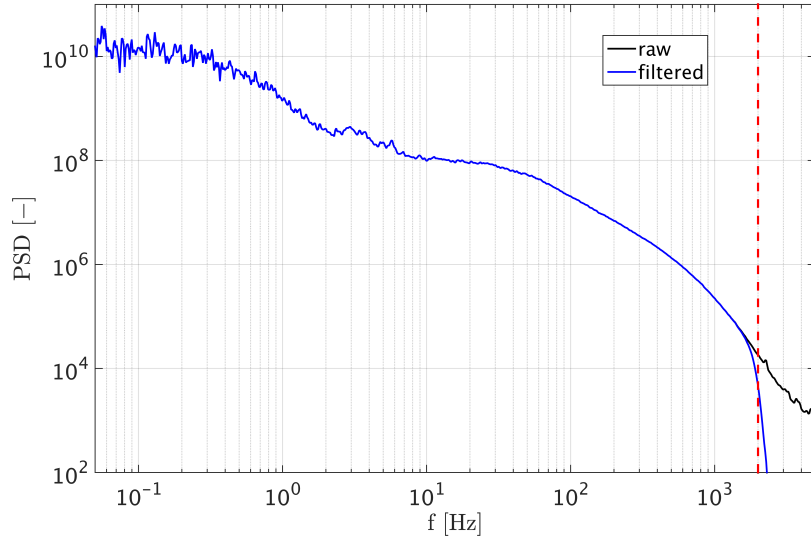


Figure 4. Power spectral density (PSD) of $u(t)$ for the intermittent inflow B. Raw data shown in black, filtered data with a 6th order Butterworth lowpass filter at $f_{\text{cut}} = 2\text{kHz}$ shown in blue. The red dashed line marks $f_{\text{cut}} = 2\text{kHz}$.

frequency for which the fluctuations of the respective turbine data are coherent with the fluctuations of the filtered velocity signal. Therefore, we consider the magnitude-squared coherence,

$$\gamma_{u'x'}^2 = \frac{|P_{u'x'}(f)|^2}{P_{u'u'}(f)P_{x'x'}(f)}, \quad (14)$$

of the filtered wind speed fluctuations and the fluctuations of the respective turbine quantity x' (Carter et al., 1973), with x being the power, torque or thrust respectively. $P_{u'x'}$ denotes the cross spectral density; $P_{u'u'}$ and $P_{x'x'}$ the auto spectrum $P_{u'u'}$ and $P_{x'x'}$ the autospectra. The results are shown in Fig. 5. At the values indicated by the red dashed lines in

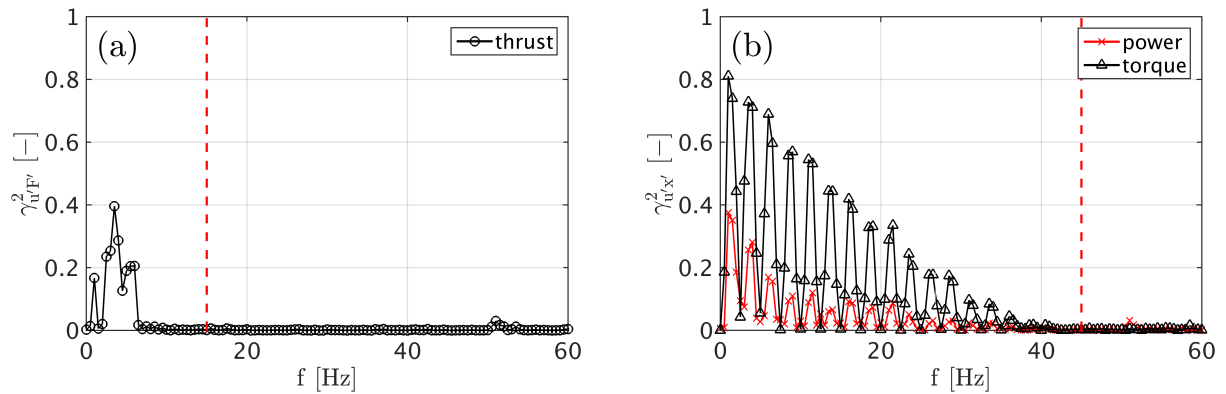


Figure 5. Magnitude-squared coherence of filtered hot wire data and thrust (a) as well as power and torque (b) respectively. 500 Hanning windows with 50 % overlap were used here, as suggested by Carter et al. (1973). Graph (b) shows regular drops of γ^2 which are caused by a filter function within the control algorithm of the model turbine. As the controller affects the electric circuit, there is a direct connection to the electric current and therewith to the power and torque. Consequently, the effect of the filter is clearly visible in this graph.

Fig. 5, the coherence of the signals is lost almost completely. Therefore, we ~~ehose~~ choose a cut off frequency of 15Hz for the thrust data and 45Hz for the power and torque data to filter the raw data using a 6th order Butterworth low pass filter. Hereby, higher frequencies are excluded, as only fluctuations resulting from the inflow should be considered. Fig. 6 shows examples of the time series of the four different signals, filtered and unfiltered. The graph in Fig. 6(a) shows the wind speed during the intermittent inflow upstream of the turbine. The other graphs show the simultaneously recorded signals of the turbine. Only the filtered data sets are used for further ~~analysis~~ analyses.

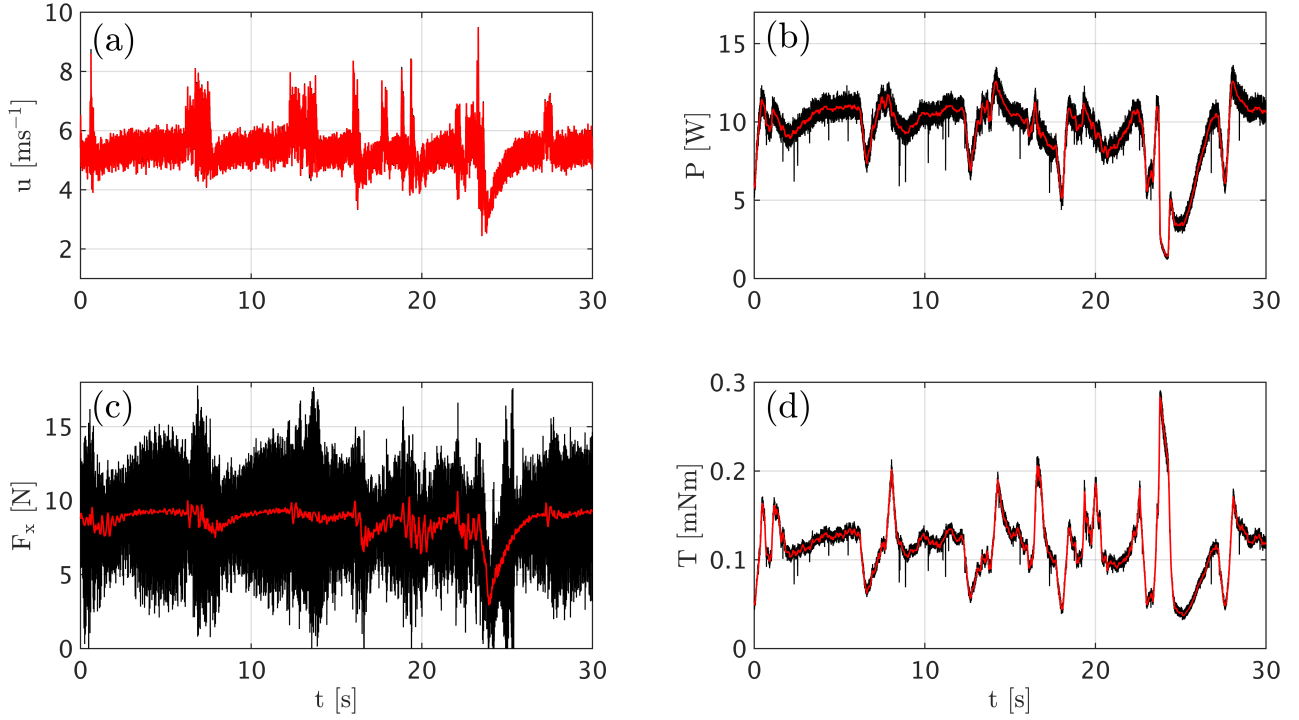


Figure 6. Original (black) and filtered (red) exemplary time series of the wind speed (a), power (b), thrust force (c) and torque (d). The wind speed was filtered using a 6th order Butterworth lowpass filter at 2kHz. In a similar way, the power and torque signals were filtered at 45Hz and the thrust force at 15Hz.

3.3 Choice of scales

As previously described, we will consider increment PDF of different time scales, $p(u_\tau)p(u_\tau)$. Defining relevant scales for WECs is not trivial and is the subject of discussion throughout the research community (van Kuik et al., 2016). Therefore, a broad spectrum of time scales was chosen, ranging from the order of seconds to the smallest scales possible while applying the described filtering. By using Taylor's hypothesis of frozen turbulence (Mathieu and Scott, 2000), the chosen time scales are related to length scales of the model turbine, with $\langle u \rangle \approx 7 \text{ m s}^{-1}$ ($\langle u \rangle \approx 7 \text{ m s}^{-1}$). The largest scale considered is $\tau = 2 \text{ s}$, which corresponds to approximately $\tau = 2 \text{ s}$. Thus, the turbine experiences a flow situation corresponding to a 14 m and is thus larger than the test section of the wind tunnel structure in the wind field having an impact on the model turbine. Smaller time scales are based on turbine lengths dimensions and the filter frequencies, respectively. Tab. 2 gives an overview of the different scales considered. When analyzing thrust data, the smallest time scale, $\tau = 25 \text{ ms}$, was excluded due to the filtering described in Sec. 3.2.

physical object	scale 1	rotor diameter scale 2	scale 3	order of blade length scale 4
time scale τ [s]	2	0.08	0.067	0.025
length/D [-]	≈ 24	1	≈ 0.8	0.3
frequency physical object	0.5	13 rotor diameter	15	40 order of blade length

Table 2. Overview of scales considered in relation to certain characteristic turbine lengths. The time scales τ were used in the analyses. To get an idea of the spatial dimension, Taylor's hypothesis is used to transfer from time to space with $\langle u \rangle \approx 7 \text{ m s}^{-1}$. The obtained length scales are expressed as multiples of the rotor diameter for better comparison. The lengths are further related to physical objects of the turbine to get a sense of the dimensions.

4 Results

4.1 Inflow

Throughout the following analysis, two different, purposely created flow situations will be considered and used as inflow conditions for the model wind turbine. Fig. 7 shows the two wind speed time series as defined in Eq. (9) with $\langle u(t) \rangle \pm \sigma_{u(t)}$ indicated. Additionally, Tab. 3 lists the mean values, standard deviations and turbulence intensities for the two cases and Fig. 8 shows a 30s excerpt. We refer to the time series as inflow A and inflow B, according to Fig. 7. It is noteworthy that in describing the wind fields by their mean values and turbulence intensities, as it is widely done, both conditions, A and B, are virtually equivalent as can be seen in Tab. 3. However, just by looking at the time series, a difference becomes

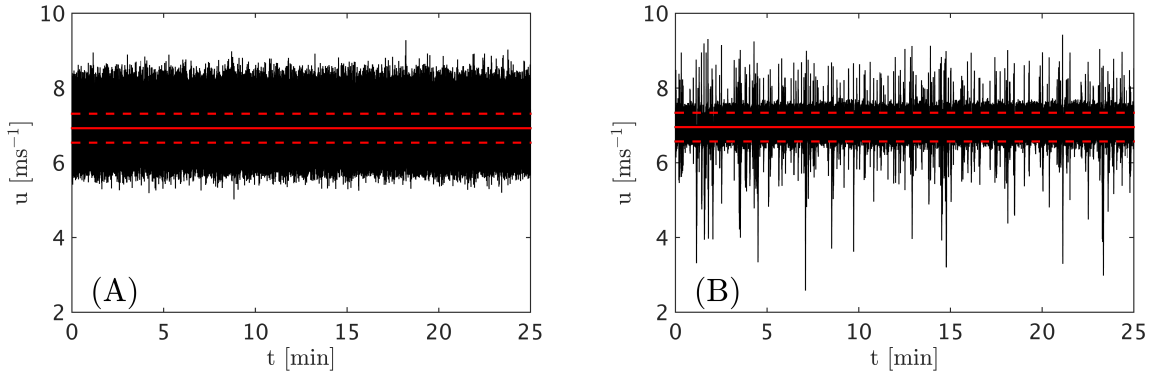


Figure 7. Velocity time series as defined in Eq. (9) of the two inflows considered, A and B. Further information is shown in Table 3. Solid red lines mark $\langle u(t) \rangle$ and dashed red lines indicate $\langle u(t) \rangle \pm \sigma_{u(t)}$.

obvious, which will be further investigated. Therefore, Fig. 9 shows the increment PDF $p(u_\tau)$ of both time series for the scales listed in Tab. 2. Clearly, both flows are significantly different regarding intermittency. While inflow A follows a Gaussian trend, inflow B shows a strongly heavy-tailed, highly intermittent distribution of increments. Therefore, extreme events

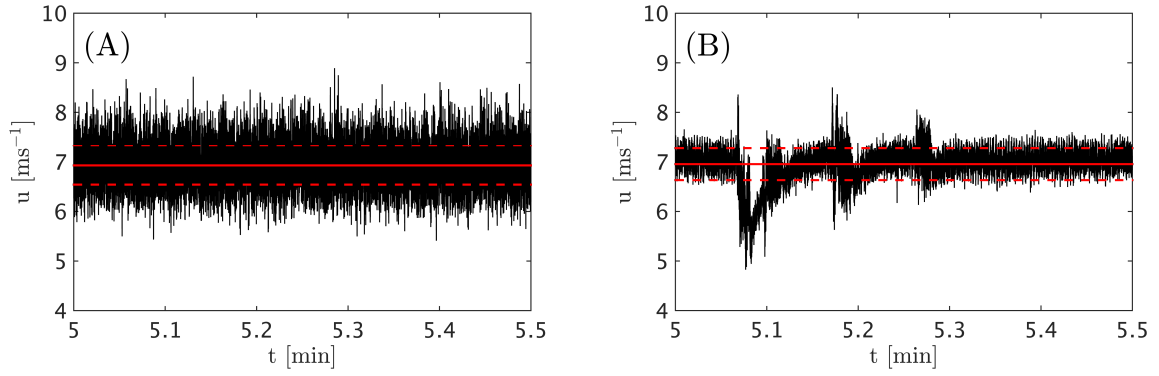


Figure 8. Excerpts of both time series shown in Fig. 7.

time series	$\langle u(t) \rangle$ [m s ⁻¹]	$\sigma_{u(t)}$ [m s ⁻¹]	TI [%]
A	6.92	0.39	5.59
B	6.96	0.38	5.50

Table 3. First two statistical moments of the time series shown in Figure 7 and their turbulence intensities. Values are rounded to two decimal places.

occur significantly more frequently in inflow B as compared to inflow A. Similar discrepancies as shown in Fig. 1 for offshore measurements and simulated data become obvious.

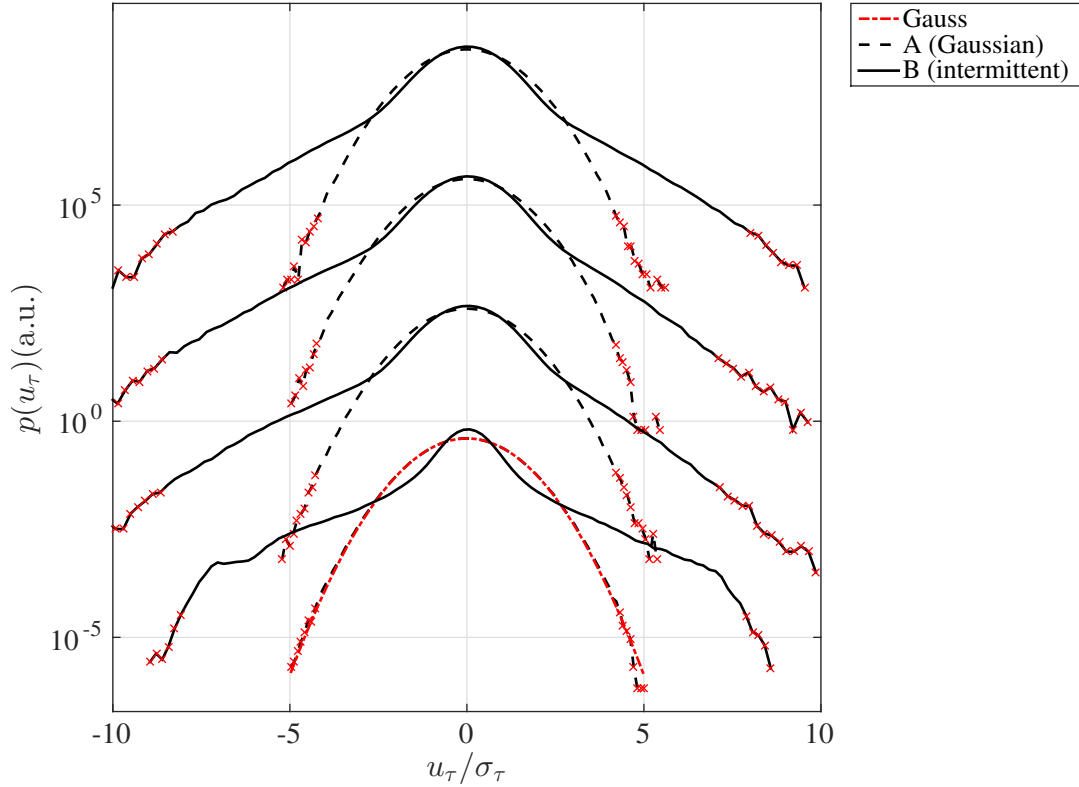


Figure 9. $p(u_\tau)$ of both velocity time series shown in Fig. 7, A (dashed) and B (solid), for $\tau = \{25 \text{ ms}, 67 \text{ ms}, 80 \text{ ms}, 2 \text{ s}\}$ from top to bottom. The different scales are shifted vertically for presentation. A Gaussian fit (dashed red line) of $p(u_{\tau=2\text{s}})$ for inflow A is added to guide the eye.

4.2 Turbine reaction

Next, we investigate the performance data of the model wind turbine when exposed to both flows A and B. To begin with, we consider the thrust force in main flow direction, $p(F_\tau)$, in Fig. 10. Clearly, the difference between Gaussian and non-Gaussian inflow conditions remains present in the thrust data for all time scales considered. Non-Gaussian **fluctuations** **increments** are not filtered **out** by the rotor. Going further, we directly compare the normalized quantities, $p(F_\tau)$ and $p(u_\tau)$ and $p(F_\tau)$ and $p(u_\tau)$, separately for both flow conditions in Fig. 11. Neither for the Gaussian nor for the intermittent case, a change in the forms of the increment PDF can be observed. Thus, we conclude that the non-Gaussian **fluctuations-character** of the inflow **are** **is** not averaged out by the rotor. In Fig. 10 and 11, the smallest time scale of $\tau = 25 \text{ ms}$ is not shown for the thrust data, as that scale interferes with the previously applied low pass filter as described in Sec. 3.2.

So far, we have considered the thrust force of the turbine as example, showing a transfer of intermittency from u_τ to F_τ u_τ to F_τ by the system dynamics of the turbine. For the power and torque we obtain similar results as for the thrust, thus we

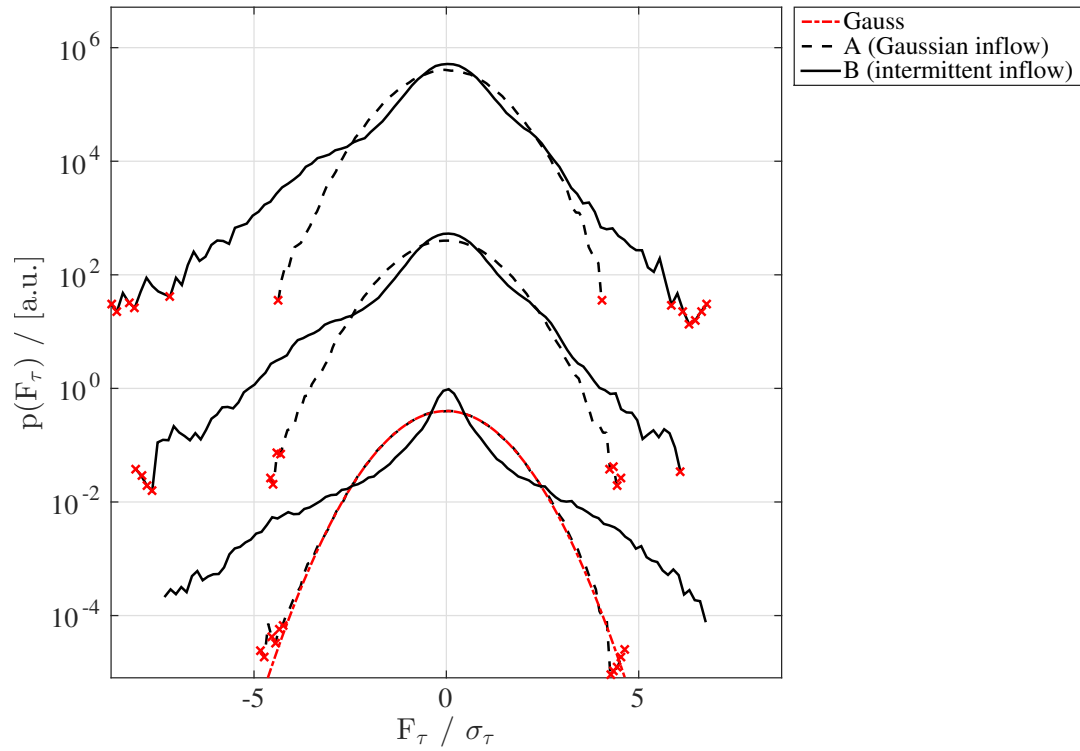


Figure 10. $p(F_\tau)$ of the turbine's thrust force (in main flow direction) exposed to the inflow conditions A (dashed) and B (solid), for $\tau = \{67 \text{ ms}, 80 \text{ ms}, 2 \text{ s}\}$ from top to bottom. The different scales are shifted vertically for presentation.

present all quantities for the intermittent inflow together in Fig. 12. None of the quantities smooth out the intermittent inflow to a close-to Gaussian distribution. Minor deviations of the respective increment PDFs are discussed in Sec. 5.

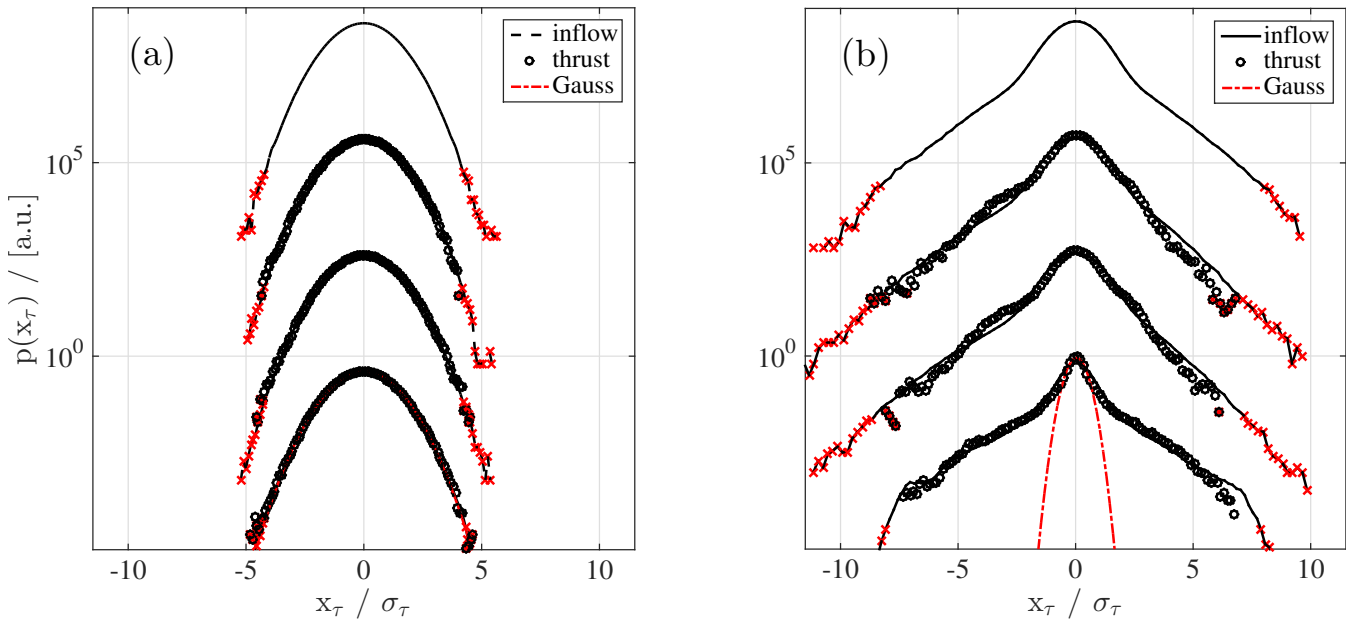


Figure 11. $p(u_\tau)$ - $p(u_\tau)$ (lines) and $p(F_\tau)$ - $p(F_\tau)$ (circles) for both inflow conditions Gaussian (a) and intermittent (b). Scales as in Fig. 10 from top to bottom $\tau = \{25 \text{ ms}, 67 \text{ ms}, 80 \text{ ms}, 2 \text{ s}\}$, shifted vertically for presentation.

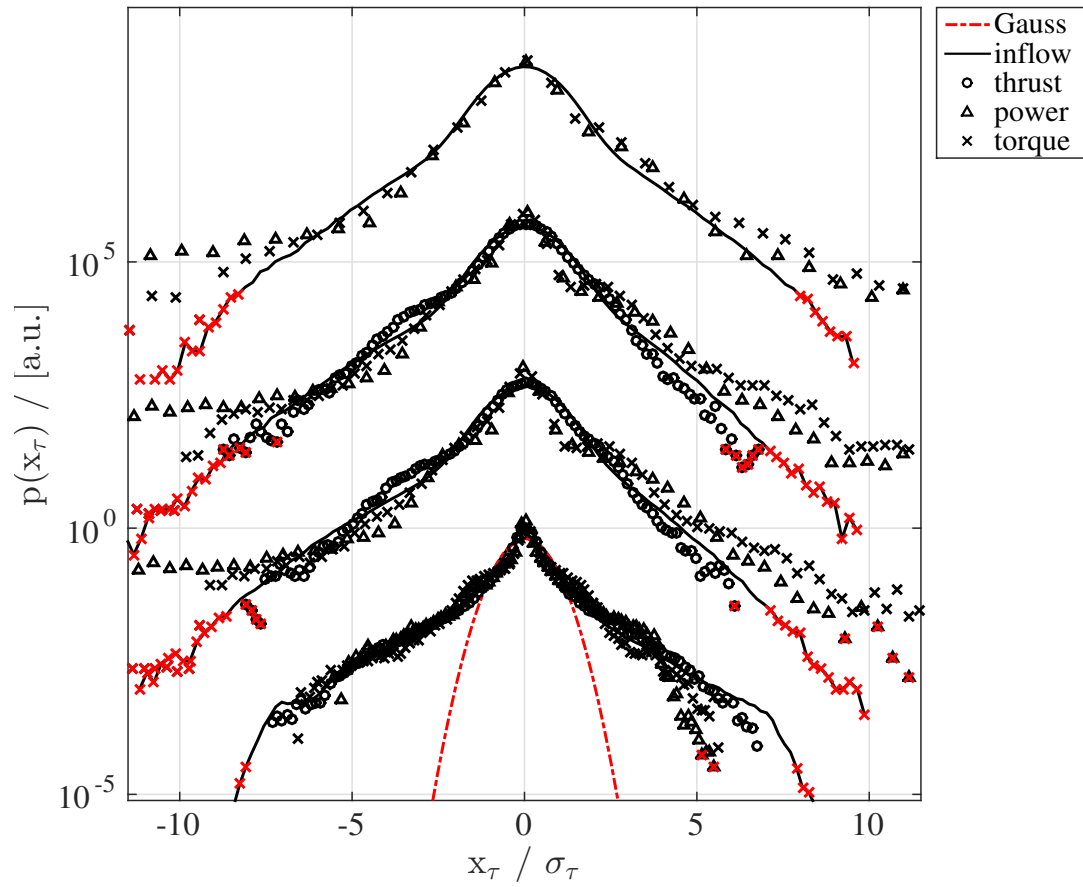


Figure 12. $p(x_\tau) / p(x_\tau)$ for the intermittent inflow condition (line, cf. Fig. 7 (aA)), thrust (circles), power (triangles) and torque (crosses). Scales as in Figure 10 from top to bottom $\tau = \{25 \text{ ms}, 67 \text{ ms}, 80 \text{ ms}, 2 \text{ s}\}$, shifted vertically for presentation.

5 Discussion

When processing the experimental data, signal fluctuations not resulting from the inflow are excluded from the analysis by previously applied low pass filters. While noise is only a minor issue considering the power and torque, the thrust data from the force balance is significantly superimposed by signal fluctuations resulting from the setup itself, cf. Fig. 6(c). These are most likely arising from vibrations of the whole setup during turbine operation, ranging from the turbine itself and the support to the fixation in the ground. Those fluctuations are of an amplitude that would influence the analysis, however, they are of higher frequency than the cut off frequency of the applied low pass filter. Therefore, they are indeed excluded from the analysis. At the same time, the procedure described in Sec. 3.2 might filter fluctuations of higher frequency than the respective cut off which are actually part of what is directly related to wind speed variations. As a result, minimal time scales have to be set, potentially excluding interesting results for smaller scales. Considering Fig. 5(a), the coherence of the hot wire signal and the thrust data is almost lost completely at approximately 10 Hz. As this corresponds to a time scale of $\tau = 0.1$ s or a length scale of 0.7 m ($\approx 1.2D \approx 1.2D$), a cutoff frequency of 15 Hz was chosen in order to include a scale between the rotor diameter and the blade length. From the analysis of other intermittent data, it can be shown that our filtering used here is not affecting the intermittency effects in a significant way. Thus, the filtering only suppresses noise effects.

Also, there might be aerodynamic effects that are of even higher frequency than the inflow fluctuations, and are therefore not captured due to the filtering. ~~As a straightforward example, a laminar flow passing a cylinder results in a well-defined frequency due to von Krmn vortex shedding, cf. Mathieu and Scott (2000). The shedding does result from the inflow, although not being related to the fluctuations. Thus, aerodynamic~~ Such effects at the rotor are possibly excluded by the low frequency filtering. This study, however, focuses on dynamics caused by the inflow turbulence.

Considering Fig. 12, some minor deviations between the increment PDF of the inflow and the turbine data can be observed. The torque and the power as defined in Eq. (12) and (11) are part of the electric circuit and therefore directly linked to the manipulative variable of the controller, being the voltage applied to the FET, $U_{FET}U_{FET}$. Thus, an analysis of those quantities includes not only fluctuations caused by the inflow, but also those resulting from the controller. As overshoots are typical for closed-loop control systems (Ogunnaike and Ray, 1994; Chien and Chung, 2003), they are much likely biasing the present analysis, especially for small time scales regarding the power and the torque. This, most likely, causes the asymmetric distributions of power and torque increments in Fig. 12. Because of that, the focus of the analysis is on the thrust data. Nonetheless, the main finding that, despite differences among the parameters, *all* quantities feature strongly intermittent distributions of increments, remains, as Fig. 12 shows.

When using the model wind turbine to grasp the impact of the different inflows considered, we do not claim full scalability. There is a Reynolds number mismatch between the scaled laboratory model and full scale turbines. Further, the model is not aero elastically scaled, which is likely to impact the scalability of the presented results. Therefore, a detailed study of the (time-) scale dependency of the results is not included here. ~~Moreover, we concentrate on the main findings of this study, being the remaining intermittency in the turbine data on the considered scales during intermittent flow conditions.~~

6 Conclusions

In this study, an experimental setup was realized, that allows the investigation of interactions between various turbulent flows with a model wind turbine. Experiments were performed in order to elaborate on the impact of non-Gaussian wind statistics on WECs. Our results ~~show no~~ do not show any filtering of the intermittent features of wind ~~speed fluctuations found in real wind~~ fields found in the atmosphere by the turbine. Consequently, one should be aware that wind characteristics, which are not reflected in standard wind field descriptions, e.g. the IEC 61400-1, have a significant impact on wind turbines. Intermittent inflow is converted to similarly intermittent turbine data on all scales considered, ranging down to sub-rotor scales. Thus, statistical properties of the inflow time series that are not captured by describing them by one-point statistics are of relevance and should be included in standards characterizing inflow conditions. If intermittent inflows lead to intermittent loading, including extreme loads that occur much more frequent than currently modeled in the standards, then this has implications for the use of the current standards in designing wind turbines to withstand the wind conditions experienced.

Appendix A: Variances of increment PDF

For completeness, the variances σ_{τ}^2 of every time series of increments, Δu_{τ} , are shown in Tab. 4 for the synthetic and offshore data, cf. Fig. 1, and for the experimental data in Tab. 5.

time scale τ [s]	1	5	10	30	60
$var(u_{\tau})$, Kaimal [$m^2 s^{-2}$]	0.25	0.47	0.53	0.58	0.58
$var(u_{\tau})$, FINO1 [$m^2 s^{-2}$]	0.04	0.11	0.15	0.24	0.31

Table 4. Variances of each increment time series $\Delta u_{\tau}(t)$, for synthetic data based on the Kaimal model and field data.

15 *Acknowledgements.* Parts of this work was funded by the Reiner Lemoine Stiftung (RLS). The authors thank Stefan Ivanell for providing the rotor blade design. Further, we thank Philip Rinn and Matthias Wächter for fruitful discussions. Finally, the authors thank the German Bundesamt für Seeschifffahrt und Hydrographie (Federal Maritime and Hydrographic Agency) and the DEWI for providing the FINO1 data.

time scale τ [s]	0.025	0.067	0.08	2
$var(u_\tau)$, Inflow A [$m^2 s^{-2}$]	0.30	0.30	0.30	0.30
$var(u_\tau)$, Inflow B [$m^2 s^{-2}$]	0.06	0.08	0.09	0.252
$var(F_\tau)$, Inflow A [$m^2 s^{-2}$]	-	0.03	0.06	0.13
$var(F_\tau)$, Inflow B [$m^2 s^{-2}$]	-	0.11	0.14	0.86
$var(P_\tau)$, Inflow A [$m^2 s^{-2}$]	0.03	0.12	0.16	3.31
$var(T_\tau)^*$, Inflow B [$m^2 s^{-2}$]	1.17	6.28	8.48	133.72

Table 5. Variances of each increment time series for the experimental data. $var(u_\tau)$ corresponds to the graphs shown in Fig. 9, $var(F_\tau)$ to the graphs in Fig. 10, $var(P_\tau)$ and $var(T_\tau)$ to $\mathfrak{p}(P_\tau)$ - $\mathfrak{p}(P_\tau)$ and $\mathfrak{p}(T_\tau)$ - $\mathfrak{p}(T_\tau)$ respectively, as shown in Fig. 12.

*) $\times 10^{-5}$.

References

- Berg, J., Natarajan, A., Mann, J., and Patton, E. G.: Gaussian vs non-Gaussian turbulence: impact on wind turbine loads, *Wind Energy*, pp. n/a–n/a, doi:10.1002/we.1963, <http://dx.doi.org/10.1002/we.1963>, we.1963, 2016.
- Boettcher, F., Renner, C., Waldl, H. P., and Peinke, J.: On the statistics of wind gusts, *Boundary-Layer Meteorology*, 108, 163–173, doi:10.1023/A:1023009722736, 2003.
- Burton, T., Sharpe, D., Jenkins, N., and Bossanyi, E.: *Wind Energy Handbook*, John Wiley and Sons, 2001.
- Carrasco, J. M., Franquelo, L. G., Bialasiewicz, J. T., Member, S., Galván, E., Guisado, R. C. P., Member, S., Ángeles, M., Prats, M., León, J. I., and Moreno-alfonso, N.: Power-Electronic Systems for the Grid Integration of Renewable Energy Sources : A Survey, *Ieee Transactions on Industrial Electronics*, 53, 1002–1016, doi:10.1109/TIE.2006.878356, 2006.
- 10 Carter, G. C., Knapp, C. H., and Nuttall, A. H.: Estimation of the Magnitude-Squared Coherence Function Via Overlapped Fast Fourier Transform Processing, *IEEE Transactions on Audio and Electroacoustics*, 21, 337–344, doi:10.1109/TAU.1973.1162496, 1973.
- Chen, Z. and Spooner, E.: Grid power quality with variable speed wind turbines, *Energy Conversion, IEEE Transactions on*, 16, 148–154, doi:10.1109/60.921466, 2001.
- Chien, I.-l. and Chung, Y.: Simple PID controller tuning method for processes with inverse response plus dead time or large overshoot response plus dead time, *Industrial & engineering ...*, pp. 4461–4477, doi:10.1021/ie020726z, <http://pubs.acs.org/doi/abs/10.1021/ie020726z>, 2003.
- De Gaetano, P., Repetto, M. P., Repetto, T., and Solari, G.: Separation and classification of extreme wind events from anemometric records, *Journal of Wind Engineering and Industrial Aerodynamics*, 126, 132–143, doi:10.1016/j.jweia.2014.01.006, <http://dx.doi.org/10.1016/j.jweia.2014.01.006><http://linkinghub.elsevier.com/retrieve/pii/S0167610514000142>, 2014.
- 20 Feng, Y., Qiu, Y., Crabtree, C. J., Long, H., and Tavner, P. J.: Monitoring wind turbine gearboxes, *Wind Energy*, 16, 728–740, doi:10.1002/we.1521, 2013.
- Frisch, U.: *Turbulence : the legacy of A.N. Kolmogorov*, vol. 1, Cambridge university press, doi:10.1017/S0022112096210791, 1995.

- Gong, K. and Chen, X.: Influence of non-Gaussian wind characteristics on wind turbine extreme response, *Engineering Structures*, 59, 727–744, doi:10.1016/j.engstruct.2013.11.029, 2014.
- International Electrotechnical Commission: IEC 61400-1: Wind turbines part 1: Design requirements, 2005.
- Jonkman, B. J.: *TurbSim user's guide: Version 1.50*, 2009.
- 5 Jonkman, J. M. and Buhl Jr, M. L.: FAST user's guide, National Renewable Energy Laboratory, Golden, CO, Technical Report No. NREL/EL-500-38230, 2005.
- Jørgensen, F. E. and Hammer, M.: Hot-wire anemometry behaviour at very high frequencies, *Measurement Science and Technology*, 8, 221–221, doi:10.1088/0957-0233/8/3/002, 1999.
- Kaimal, J. C. J., Wyngaard, J. C. J., Izumi, Y., Coté, O. R., and Cote, O. R.: Spectral Characteristics of Surface-Layer Turbulence, *Quarterly Journal of the ...*, 98, 563–589, doi:10.1002/qj.49709841707, 1972.
- 10 Larsen, T. J. and Hansen, A. M.: *How 2 HAWC2, the user's manual*, Risø National Laboratory, 2007.
- Liu, L., Hu, F., Cheng, X.-L., and Song, L.-L.: Probability Density Functions of Velocity Increments in the Atmospheric Boundary Layer, *Boundary-Layer Meteorology*, 134, 243–255, doi:10.1007/s10546-009-9441-z, 2010.
- Mathieu, J. and Scott, J.: *An introduction to turbulent flow*, Cambridge University Press, 2000.
- 15 Milan, P., Wächter, M., and Peinke, J.: Turbulent Character of Wind Energy, *Phys. Rev. Lett.*, 110, 138 701, doi:10.1103/PhysRevLett.110.138701, <http://link.aps.org/doi/10.1103/PhysRevLett.110.138701>, 2013.
- Morales, A., Wächter, M., and Peinke, J.: Characterization of wind turbulence by higher-order statistics, *Wind Energy*, 15, 391–406, doi:10.1002/we.478, 2012.
- Moriarty, P. J. and Hansen, A. C.: *AeroDyn theory manual*, Citeseer, 2005.
- 20 Musial, W., Butterfield, S., and McNiff, B.: Improving Wind Turbine Gearbox Reliability Preprint, European Wind Energy Conference, pp. 1–13, 2007.
- Mücke, T., Kleinhans, D., and Peinke, J.: Atmospheric turbulence and its influence on the alternating loads on wind turbines, *Wind Energy*, 14, 301–316, doi:10.1002/we.422, <http://dx.doi.org/10.1002/we.422>, 2011.
- Nielsen, M., Larsen, G., and Hansen, K.: Simulation of inhomogeneous, non-stationary and non-Gaussian turbulent winds, *Journal of Physics: Conference Series*, 75, 12 060, doi:10.1088/1742-6596/75/1/012060, <http://stacks.iop.org/1742-6596/75/i=1/a=012060>, 2007.
- 25 Odemark, Y.: *Wakes behind wind turbines-Studies on tip vortex evolution and stability*, 2012.
- Ogunnaike, B. A. and Ray, W. H.: *Process dynamics, modeling, and control*, vol. 1, Oxford University Press New York, 1994.
- Press, W. H., Teukolsky, S. A., Vetterling, W. T., and Flannery, B. P.: *Numerical Recipes in C (2Nd Ed.): The Art of Scientific Computing*, Cambridge University Press, New York, NY, USA, 1992.
- 30 Reinke, N., Homeyer, T., Hölling, M., and Peinke, J.: Flow Modulation by an Active Grid, *Experiments in Fluids*, submitted, 2016.
- Schlipf, D., Schlipf, D. J., and Kühn, M.: Nonlinear model predictive control of wind turbines using LIDAR, *Wind Energy*, 16, 1107–1129, doi:10.1002/we.1533, <http://doi.wiley.com/10.1002/we.1533>, 2013.
- Schottler, J., Hölling, A., Peinke, J., and Hölling, M.: Design and implementation of a controllable model wind turbine for experimental studies, *Journal of Physics: Conference Series*, 753, 072 030, doi:10.1088/1742-6596/753/7/072030, <http://stacks.iop.org/1742-6596/753/i=7/a=072030?key=crossref.34e2c393ad63869d0a600bad3c2c4d9a>, 2016.
- 35 Sørensen, P., Cutululis, N. A., Viguera-Rodríguez, A., Jensen, L. E., Hjerrild, J., Donovan, M. H., and Madsen, H.: Power Fluctuations From Large Wind Farms, *IEEE Transactions on Power Systems*, 22, 958–965, doi:10.1109/TPWRS.2007.901615, 2007.

- van Kuik, G. A. M., Peinke, J., Nijssen, R., Lekou, D., Mann, J., Sørensen, J. N., Ferreira, C., van Wingerden, J. W., Schlipf, D., Gebraad, P., Polinder, H., Abrahamsen, A., van Bussel, G. J. W., Sørensen, J. D., Tavner, P., Bottasso, C. L., Muskulus, M., Matha, D., Lindeboom, H. J., Degraer, S., Kramer, O., Lehnhoff, S., Sonnenschein, M., Sørensen, P. E., Künneke, R. W., Morthorst, P. E., and Skytte, K.: Long-term research challenges in wind energy – a research agenda by the European Academy of Wind Energy, *Wind Energy Science*, 1, 1–39, doi:10.5194/wes-1-1-2016, <http://www.wind-energ-sci.net/1/1/2016/>, 2016.
- 5 Weitemeyer, S., Reinke, N., Peinke, J., and Hölling, M.: Multi-scale generation of turbulence with fractal grids and an active grid, *Fluid Dynamics Research*, 45, 061407, doi:10.1088/0169-5983/45/6/061407, <http://stacks.iop.org/1873-7005/45/i=6/a=061407?key=crossref.8476ac727119acae00736461833aca18>, 2013.
- Westerhellweg, A., Neumann, T., and Riedel, V.: Fino1 mast correction, *Dewi magazin*, 40, 3, 2012.
- 10 Wächter, M., Heißelmann, H., Hölling, M., Morales, A., Milan, P., Mücke, T., Peinke, J., Reinke, N., and Rinn, P.: The turbulent nature of the atmospheric boundary layer and its impact on the wind energy conversion process, *Journal of Turbulence*, 13, N26, doi:10.1080/14685248.2012.696118, <http://dx.doi.org/10.1080/14685248.2012.696118>, 2012.